

Efficient Light-Dependent DNA Repair Requires a Large Cofactor Separation

Robert Epple and Thomas Carell*

Contribution from the Laboratorium für Organische Chemie, Eidgenössische Technische Hochschule, Universitätstrasse 16, CH-8092 Zürich, Switzerland

Received February 15, 1999

Abstract: DNA photolyases are repair enzymes which split (repair) UV-induced cyclobutane DNA lesions. Critical steps in the light-driven repair reaction are the absorption of light by a deazaflavin or methenyl tetrahydrofolate cofactor and the transfer of the excitation energy to a reduced and deprotonated FADH⁻ cofactor, which initiates an electron transfer to the dimer lesion. Although most efficient energy transfer requires a close cofactor arrangement, there is a separation of > 17 Å between the cofactors in photolyases. To determine the effect of the large cofactor distance on the repair efficiency, a systematic study with model compounds was performed. A series of compounds were synthesized which contain a model DNA lesion covalently connected to a flavin and a deazaflavin. While the flavin–dimer lesion distance was kept constant in all model compounds, the flavin–deazaflavin distance was incrementally increased. Investigation of the dimer cleavage efficiency shows that compounds with a large cofactor separation possess a low energy-transfer efficiency but split the dimer most efficiently within a few minutes. Model compounds with a close cofactor orientation feature a highly efficient energy transfer from the deazaflavin to the flavin. They are, however, unable to perform the repair of the dimer lesion. At very short cofactor distances, the light-driven repair process is fully inhibited. This is explained by a competitive electron transfer between both cofactors, which hinders the electron transfer to the dimer lesion and hence the dimer splitting. The presented data suggest that the large cofactor separation (17 Å) found in photolyases is a critical parameter that determines the DNA repair efficiency by photolyases.

Introduction

Photoinduced electron-transfer reactions play a key role in biology.^{1,2} They are the basis for the photosynthetic process in which chlorin, pheophytin, and quinone chromophores orchestrate the conversion of sunlight into chemical energy.^{3,4} Photolyase DNA repair enzymes utilize a reduced riboflavin (FADH⁻), a ribodeazaflavin (F₀), or a methenyl tetrahydrofolate (MTHF) for the catalytic, light-dependent repair of the most abundant UV-induced genome lesions.^{5–7} A similar set of cofactors was recently discovered in cryptochrome photoreceptors,⁸ which control key developmental events in plants, such as hypocotyl elongation,⁹ and also set the circadian clock.¹⁰ DNA photolyases are repair enzymes that represent a major

defense system against UV-induced DNA damage in many organisms.^{11,12}

UV irradiation of cells induces a [2π + 2π] cycloaddition of pyrimidines located above each other in the DNA double strand. The resulting *cis*–*syn* pyrimidine dimers are responsible for cell death and the degeneration of cells into tumor cells.^{13,14} DNA photolyases specifically recognize the *cis*–*syn* dimer lesions and split the dimers in a light-dependent reaction.¹⁵ The key mechanistic steps of the repair reaction are depicted in Figure 1.

The repair mechanism of F₀-containing photolyases (type II) includes the absorption of light by the F₀ cofactor and an energy transfer from the F₀ to a reduced and deprotonated FADH⁻.^{16–18} The flavin donates an electron to the cyclobutane pyrimidine dimer lesion, which cleaves spontaneously as its radical anion.⁶ Two recent X-ray crystal structures of photolyases reveal a large distance between the light-harvesting and the redox-active cofactor.^{19,20} Despite their need to interact efficiently, the cofactors were found to be separated by more than 17 Å, which

* To whom correspondence should be addressed. Tel.: 0041-1-632-2944. Fax: 0041-1-632-1109. E-mail: tcarell@org.chem.ethz.ch.

(1) Gray, H. B.; Winkler, J. R. *Annu. Rev. Biochem.* **1996**, *65*, 537–561.

(2) Langen, R.; Chang, I.-J.; Germanas, J. P.; Richards, J. H.; Winkler, J. R.; Gray, H. B. *Science* **1995**, *268*, 1733–1735.

(3) Clayton, R. K. *Photosynthesis: Physical Mechanisms and Chemical Patterns*; Cambridge University Press: London, 1980.

(4) Wasielewski, M. R. *Chem. Rev.* **1992**, *92*, 435–461. Kurreck, H.; Huber, M. *Angew. Chem., Int. Ed. Engl.* **1995**, *34*, 849–866.

(5) Sancar, A. *Biochemistry* **1994**, *33*, 2–9.

(6) Heelis, P. F.; Hartman, R. F.; Rose, S. D. *Chem. Soc. Rev.* **1995**, *289*–297.

(7) Begley, T. P. *Acc. Chem. Res.* **1994**, *27*, 394–401. Carell, T.; Epple, R. *Eur. J. Org. Chem.* **1998**, *1245*, 5–1258.

(8) Ahmad, M.; Cashmore, A. R. *Nature* **1993**, *366*, 162–166.

(9) Malhotra, K.; Kim, S.-T.; Batschauer, A.; Dawut, L.; Sancar, A. *Biochemistry* **1995**, *34*, 6892–6899.

(10) Miyamoto, Y.; Sancar, A. *Proc. Natl. Acad. Sci. U.S.A.* **1998**, *95*, 6097–6102.

(11) Friedberg, E. C.; Walker, G. C.; Siede, W. *DNA repair and mutagenesis*; ASM Press: Washington, DC, 1995.

(12) Carell, T. *Chimia* **1995**, *49*, 365–373.

(13) Taylor, J.-S. *J. Chem. Educ.* **1990**, *67*, 835–841.

(14) Taylor, J.-S. *Acc. Chem. Res.* **1994**, *27*, 76–82.

(15) Carell, T. *Angew. Chem., Int. Ed. Engl.* **1995**, *34*, 2491–2494.

(16) Kim, S.-T.; Heelis, P. F.; Okamura, T.; Hirata, Y.; Mataga, N.; Sancar, A. *Biochemistry* **1991**, *30*, 11262–11270.

(17) Kim, S.-T.; Heelis, P. F.; Sancar, A. *Biochemistry* **1992**, *31*, 11244–11248.

(18) Jorns, M. S.; Ramsey, A. J. *Biochemistry* **1992**, *31*, 8437–8441.

(19) Park, H.-W.; Kim, S.-T.; Sancar, A.; Deisenhofer, J. *Science* **1995**, *268*, 1866–1872.

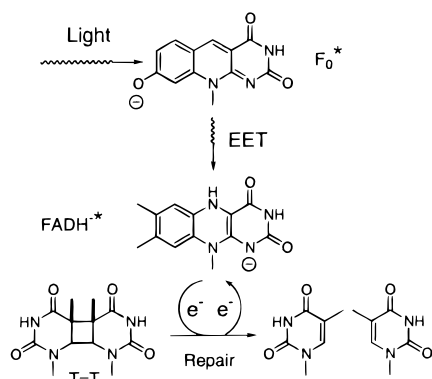


Figure 1. Schematic representation of the mechanism of the type II photolyase-initiated DNA repair process. The deazaflavin (F_0) absorbs light and transfers the energy to a reduced and deprotonated flavin ($FADH^-$). This initiates an electron transfer to a cyclobutane pyrimidine dimer lesion ($T=T$). The dimer cleaves spontaneously as its radical anion. EET = Excitation energy transfer.

led to the hypothesis that the cofactor–cofactor interaction has never been optimized during evolution.^{19,21} Moreover, two invariant basic amino acid residues at the bottom of the F_0 binding pocket in all type II photolyases ensure the deprotonation of the F_0 cofactor (O^- state) for an unknown reason.²⁰

We recently communicated the synthesis of chimaeric flavin- and deazaflavin-containing pyrimidine dimer model compounds,^{22–24} which are able to mimic the $F_0 \rightarrow FADH^-$ energy transfer and the $FADH^- \rightarrow$ dimer electron-transfer process of the photolyase repair reaction.²⁵ In this publication, we report the investigation of the potential reasons for the structural peculiarities found in photolyases. With the set of novel bis-cofactor model compounds presented in Scheme 1, the effects of the cofactor–cofactor distance and the deazaflavin deprotonation on the energy-transfer efficiency and repair rate were studied. All model systems contain a flavin (Fl) and a deazaflavin (dFl) covalently attached to a *cis-syn*-cyclobutane uracil dimer.²⁶ The flavin–dimer distance was kept constant in all model compounds, which ensures a constant electron-transfer efficiency from the flavin to the dimer, while the flavin–deazaflavin distance was systematically changed. The distance is shortest in the model compounds **1a** and **1b** and largest in the model compounds **2a** and **2b**, which contain four “semirigid” proline spacers.^{27,28} In all model compounds of series a (**1a–4a**), the deazaflavin is fixed in the OH form due to benzylation of the 8-OH group. Cleavage of this protection group by catalytic hydrogenation and adjustment of the pH to >8 converted the deazaflavin ($pK_a \approx 6$)²⁹ into the deprotonated form present in **1b–4b** (series b). This “quinoid” deazaflavin is the

active form in type II DNA photolyases. Comparison of the cleavage results for all model compounds allowed the determination of two main parameters. It was found that the flavin–deazaflavin distance strongly influences the repair rate in a counterintuitive way, and we could determine that the deprotonation of the deazaflavin helps to increase the repair efficiency.

Results and Discussion

Synthesis of the Model Compounds. All model compounds **1a/b–4a/b** and **5** were chemically assembled, as depicted in Scheme 1, from the cyclobutane uracil dimer building block **6** and the *N*(3)-alkyl-*N*(10)-aminoethylflavins **7** and **8**, the flavin amino acid **9**, the *N*(3)-pentyl-*N*(10)-aminoethyldeazaflavin **10**, and the deazaflavin amino acid **11** (Schemes 2 and 3). The synthesis of the uracil dimer **6**, of the flavin **8**, and of the reference model compound **5** was achieved as recently described in detail.^{26,30} All other cofactor derivatives were prepared as depicted in Schemes 2 and 3. The flavin and the deazaflavin peptides **12–14**, required for the preparation of the model compounds **1–3**, were prepared by liquid- and solid-phase peptide synthesis (Scheme 4).³¹

For the preparation of the flavin amino acid **9** and the pentyl-substituted flavin **7** (Scheme 2), the *tert*-butyloxycarbonyl (Boc)-protected aminoethyl-substituted flavin **15**³² was alkylated with *tert*-butyl bromoacetate to give the Boc-protected flavin amino acid *tert*-butyl ester **16**. Acidic cleavage of the *tert*-butyl-containing protection groups yielded the flavin amino acid **17**, which was converted into the fluorenylmethoxycarbonyl (Fmoc)-protected amino acid **9**, ready for the incorporation into peptides using solid-phase synthesis, by treatment with *N*-(9-fluorenylmethoxycarbonyloxy)succinimide (Fmoc-OSu) and K_2CO_3 . Alkylation of **15** with pentyl bromide in dimethylformamide (DMF) with CS_2CO_3 as the base afforded the pentyl-substituted flavin derivative **18**, which was deprotected with trifluoroacetic acid (TFA) to give **7**.

The deazaflavins **10** and **11** (Scheme 3) were prepared by substitution of 6-chlorouracil **19** with the mono-Boc-protected ethylenediamine **20**.³³ The product **21** was condensed to the deazaflavin **22** with 2,4-(dibenzoyloxy)benzaldehyde (**23**).³⁴ Alkylation of the deazaflavin **22** with pentyl bromide in the presence of CS_2CO_3 in DMF yielded the pentyl-substituted deazaflavin **24**. Cleavage of the Boc group with TFA afforded **10**. Alkylation of **22** with *tert*-butyl bromoacetate to **25** and acidic cleavage of the *tert*-butyl-containing protecting groups yielded the deazaflavin amino acid **26**. Reaction of **26** with Fmoc-OSu and K_2CO_3 furnished the deazaflavin amino acid **11**, ready for incorporation into peptides using solid-phase synthesis.

For the synthesis of the flavin–deazaflavin peptide **12** (Scheme 4), the carboxylic acid **9** was activated with benzo-triazol-1-yloxytris(dimethylamino)phosphoniumhexafluorophosphate (BOP) and reacted with the *N*(3)-pentyl-substituted deazaflavin **10** in DMF to yield **27**. Cleavage of the Fmoc group in **27** was performed with diethylamine directly before the coupling with the dimer diacid **6**, without purification and characterization of the intermediate amine **12**.

(20) Tamada, T.; Kitadokoro, K.; Higuchi, Y.; Inaka, K.; Yasui, A.; de Ruiter, P. E.; Eker, A. P. M.; Miki, K. *Nature Struct. Biol.* **1997**, *11*, 887–891.

(21) Heelis, P. F. *J. Photochem. Photobiol., B* **1997**, *38*, 31–34.

(22) Eker, A. P. M.; Dekker, R. H.; Berends, W. *Photochem. Photobiol.* **1981**, *33*, 65.

(23) Rokita, S. E.; Walsh, C. T. *J. Am. Chem. Soc.* **1984**, *106*, 4589–4595.

(24) Jorns, M. S. *J. Am. Chem. Soc.* **1987**, *109*, 3133–3136.

(25) Epple, R.; Carell, T. *Angew. Chem., Int. Ed. Engl.* **1998**, *37*, 938–941.

(26) Carell, T.; Epple, R.; Gramlich, V. *Helv. Chim. Acta* **1997**, *80*, 2191–2203.

(27) McCafferty, D. G.; Friesen, D. A.; Danielson, E.; Wall, C. G.; Saderholm, M. J.; Erickson, B. W.; Meyer, T. J. *Proc. Natl. Acad. Sci. U.S.A.* **1996**, *93*, 8200–8204.

(28) Slate, C. A.; Striplin, D. R.; Moss, J. A.; Chen, P.; Erickson, B. W.; Meyer, T. J. *J. Am. Chem. Soc.* **1998**, *120*, 4885–4886.

(29) Walsh, C. *Acc. Chem. Res.* **1986**, *19*, 216–221.

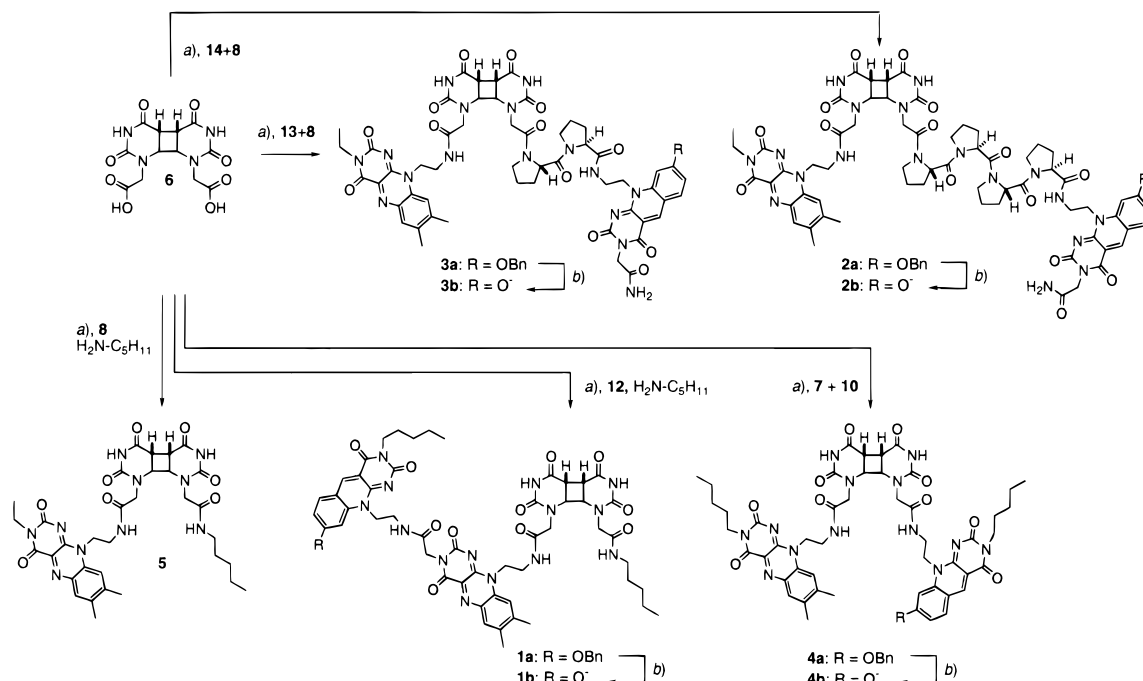
(30) Epple, R.; Wallenborn, E.-U.; Carell, T. *J. Am. Chem. Soc.* **1997**, *119*, 7440–7451.

(31) Carell, T.; Schmid, H.; Reinhard, M. *J. Org. Chem.* **1998**, *63*, 8741–8747.

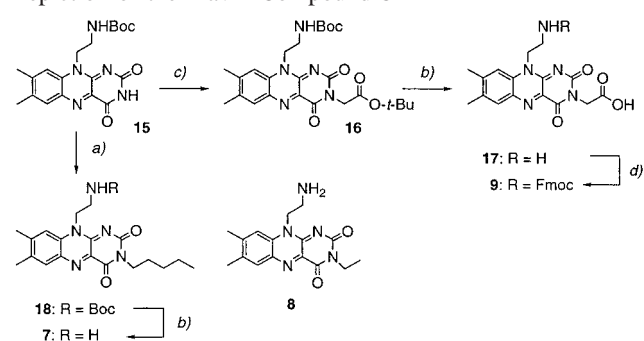
(32) Butenandt, J.; Eker, A. P. M.; Epple, R.; Gramlich, V.; Wallenborn, E.-U.; Carell, T. *Chem. Eur. J.*, accepted for publication.

(33) Pfeleiderer, W.; Nübel, G. *Liebigs. Ann. Chem.* **1959**, *631*, 168–174. Petry, C., Dissertation, Heidelberg, 1993.

(34) Kimachi, T.; Tanaka, K.; Yoneda, F. *J. Heterocycl. Chem.* **1991**, *28*, 439–443.

Scheme 1. Synthesis of the Model Compounds **5** and **1a/b** to **4a/b**^a

^a Conditions: (a) BOP, NEt₃, DMF, room temperature; (b) H₂, Pd/BaSO₄, acetic acid, room temperature.

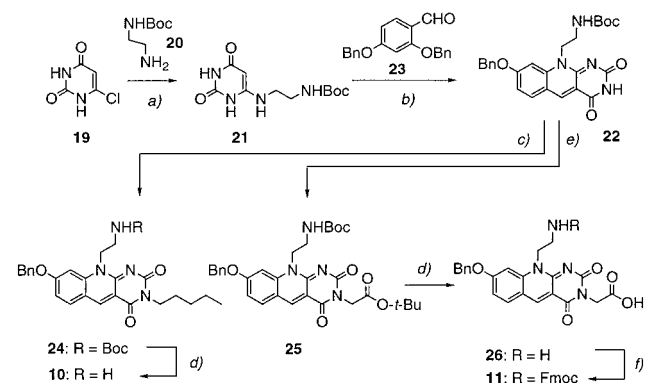
Scheme 2. Synthesis of the Flavin Building Blocks **7** and **9** Required for the Preparation of the Model Compounds: Depiction of the Flavin Compound **8**^a

^a Conditions: (a) Br-C₅H₁₁, DMF, Cs₂CO₃; (b) TFA; (c) Br-CH₂-COO-*t*-Bu, Cs₂CO₃, DMF; (d) Fmoc-OSu, K₂CO₃, 4 °C.

The synthesis of the deazaflavin peptides **13** and **14** required coupling of the deazaflavin amino acid **11** to a Rink-Amide MBHA resin to yield the resin **28**.³⁵ This was performed in 1-methyl-2-pyrrolidone (NMP) as the solvent, with diisopropylethylamine (DIEA) as the base, after in situ activation of the carboxylic acid group of **11** with *N*-hydroxybenzotriazole/2-(1*H*-benzotriazol-1-yl)-1,1,3,3-tetramethyluronium tetrafluoroborate (HOBT/TBTU).³⁶ Subsequent cleavage of the Fmoc protection group with piperidine in DMF and stepwise coupling of either two or four Fmoc-protected proline units to the deazaflavin-loaded resin **28** gave the resins **29** and **30**, respectively. The final cleavage of the Fmoc group in **29** and **30** with piperidine and of the peptides from the resins with TFA afforded the crude peptides **13** and **14**. Both peptides were obtained after reversed-phase HPLC purification in excellent yields and purity as yellow powders.

(35) Grant, G. A. *Synthetic Peptides: A User's Guide*; W. H. Freeman and Co.: New York, 1992.

(36) Knorr, R.; Trzeciak, A.; Bannwarth, W.; Gillissen, D. *Tetrahedron Lett.* **1989**, 30, 1927–1930.

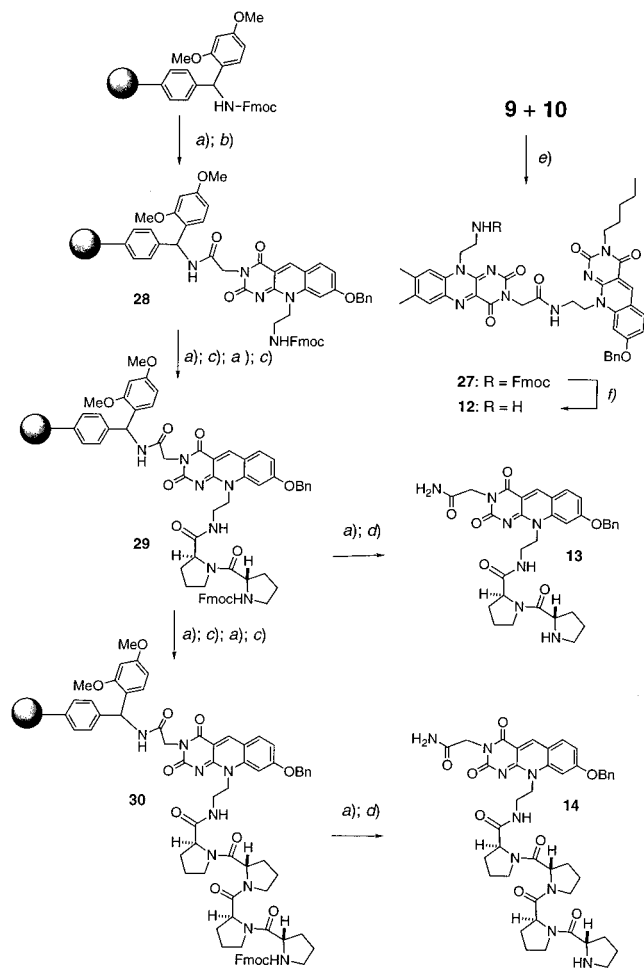
Scheme 3. Synthesis of the Deazaflavin Building Blocks **10** and **11**^a

^a Conditions: (a) *n*-butanol, reflux; (b) DMF, 120 °C, 20 h; (c) Br-C₅H₁₁, DMF, Cs₂CO₃; (d) TFA; (e) Br-CH₂-COO-*t*-Bu, Cs₂CO₃, DMF; (f) Fmoc-OSu, K₂CO₃, 4 °C.

The synthesis of the model compounds (Scheme 1) required activation of the two carboxylic acid groups of **6** with BOP in DMF.³⁷ After addition of 1 equiv of the building blocks **8** or **12** and DIEA, the mixture was allowed to react for 1 h. Subsequent addition of an excess of pentylamine yielded the model compounds **5** and **1a**, respectively. Reaction of the BOP-activated uracil dimer **6** with 1 equiv of the deazaflavin peptides **13** or **14**, followed by addition of the flavin **8**, furnished the model compounds **2a** and **3a**. Reaction of the BOP-activated uracil dimer **6** with the pentyl-substituted flavin **7**, followed by addition of the deazaflavin **10**, yielded the model compound **4a**. All model compounds were isolated either by flash chromatography (**5**, **1a**, and **4a**) on silica-*H* or by preparative reversed-phase HPLC on a C18-column with a water/acetonitrile gradient (**2a**, **3a**). The compounds were obtained as yellow powders. For the synthesis of the model compound in series b (**1b–4b**), which possess a debenzylated “quinoid” deazaflavin, the corresponding

(37) Castro, B.; Evin, G.; Delve, C.; Seyer, R. *Synthesis* **1977**, 413–469.

Scheme 4. Synthesis of the Flavin–Deazaflavin Peptide **12** Needed for the Preparation of the Model Compounds **1a** and **1b** and of the Deazaflavin–Proline Peptides **13** and **14** Required for the Preparation of the Model Compounds **2a/b** and **3a/b**^a



^a Conditions: (a) 20% piperidine in DMF; (b) **11**, HOBT, TBTU, DIEA; (c) Fmoc-Pro, HOBT, TBTU, DIEA; (d) TFA/H₂O/triisopropylsilane (TIS) (95:2.5:2.5), 1 h; (e) BOP, NEt₃, DMF; (f) 40% Me₂NH in H₂O, DMF, 20 min.

model compounds **1a–4a** were dissolved in acetic acid. A small amount of Pd/BaSO₄ catalyst was added, and the suspension was stirred under a hydrogen atmosphere until complete debenzoylation was achieved. During the hydrogenolysis, both chromophores were reduced as well. Stirring of the reaction solution in air, however, caused complete reoxidation of the flavin and the deazaflavin cofactors. Decomposition of the model compounds was not observed (thin-layer chromatography). The model compound **4b** was prepared in quantitative yield on a larger scale to allow its isolation and complete characterization. All other model compounds **1b–3b** were characterized by UV and fluorescence spectroscopy without prior purification. The purity of the prepared model compounds **1b–3b** was determined by analytical reversed-phase HPLC before the measurements and found to be >96%.

Sample Preparation. To quantify the efficiency of the dimer splitting in all model compounds **1a/b–4a/b**, selective reduction of the flavin unit in the presence of a deazaflavin chromophore either in its OBn[−] or its “quinoid” O[−] form had to be performed. This was accomplished with sodium dithionite. The model compounds were dissolved (10^{−5}–10^{−6} M) in ethylene glycol (3 mL) in a UV cuvette, stoppered with a rubber septum, and

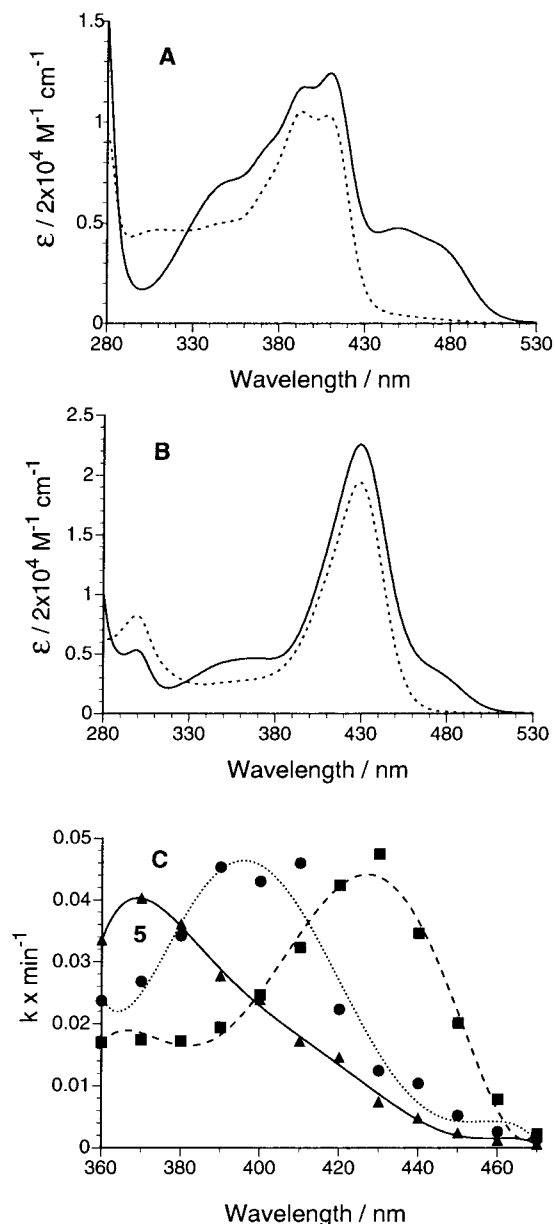


Figure 2. (A) UV spectra of the model compounds **1a–4a** (series a) prior to the reduction with dithionite (solid line) and after the addition of sodium dithionite (dotted line). (B) UV spectra of the model compounds **1b–4b** (series b) prior to the reduction with dithionite (solid line) and after the addition of sodium dithionite (dotted line). All UV data were recorded at 10^{−5} M in ethylene glycol. (C) Action spectra of the reference compound **5** (\blacktriangle), of the model compounds in series a (\bullet , represented by **4a**), and of the model compounds of series b (\blacksquare , represented by **4b**).

DIEA (10 μ L) was added to ensure basic conditions. The assay solution was subsequently purged with nitrogen. The dithionite solution was then carefully added with a microsyringe until all flavin was reduced. The selective reduction could be monitored by UV spectroscopy (Figure 2A,B). The nonreduced model compounds in series a possess absorption bands around 390 and 410 nm, due to the benzylated deazaflavin chromophore (Figure 2A). The oxidized flavin possesses absorption maxima at 350 and 450 nm.^{38–40} In the reduced state, the absorption around 450 nm disappears, and the absorption at 350 nm is

(38) Bruce, T. C. *Acc. Chem. Res.* **1980**, *13*, 256–262.

(39) Walsh, C. *Acc. Chem. Res.* **1980**, *13*, 148–155.

(40) Dudley, K. H.; Ehrenberg, A.; Hemmerich, P.; Müller, F. *Helv. Chim. Acta* **1964**, *47*, 1354–1383.

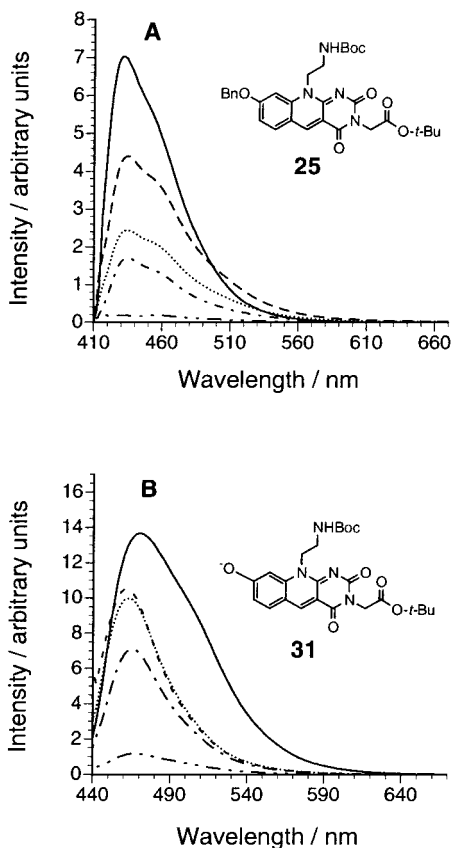


Figure 3. (A) Fluorescence spectra of the reference compound **25** (—) and of the model compounds **1a–4a** (**1a**, ·····; **4a**, - - -; **3a**, ···; **2a**, - - -). (B) Fluorescence spectra of the reference compound **31** (—) and of the model compounds **1b–4b** (**1b**, ·····; **4b**, - - -; **3b**, ···; **2b**, - - -). All fluorescence spectra were recorded in ethylene glycol at 10^{-6} M concentration.

strongly reduced. The absorption bands of the deazaflavin unit, however, remain intact, indicating the successful reduction of only the flavin unit. Figure 2B shows the reduction of the model compounds of series b. These model compounds possess a “quinoid” deazaflavin, which absorbs most intensely at 430 nm. Again, only the absorption around 450 nm of the oxidized flavin disappears upon addition of the dithionite solution. The absorption at 430 nm remains, which proves that the “quinoid” deazaflavin stays in its oxidized state. The obtained UV spectra of the reduced solutions of all series b model compounds are in perfect agreement with the UV data of type II DNA photolyases in the active state.⁴¹ This result underlines that these model compounds perfectly simulate the spectroscopic properties of these enzymes.^{41,42}

dFl → FlH⁻ Energy-Transfer Efficiency. The efficiency of the dFl → FlH⁻ energy transfer was investigated in all model compounds using steady-state fluorescence spectroscopy (Figure 3A,B). The benzylated deazaflavins exhibit a strong fluorescence at 430 nm (Figure 3A). All model compounds in series b possess a strong fluorescence band at 470 nm (Figure 3B). If energy donation from the deazaflavin chromophore to an energy acceptor occurs, this is expected to lead to a quenching of the deazaflavin fluorescence. Increasing energy-transfer efficiency should yield decreasing fluorescence intensities.⁴³ The fluores-

cence data of all model compounds **1–4** clearly show a strongly reduced deazaflavin fluorescence in all model compounds, compared to the reference deazaflavins **25** and **31**. In agreement with the r^{-6} distance dependence of energy-transfer rates, according to Förster theory,⁴⁴ we observe the strongest fluorescence reduction (95% deazaflavin fluorescence quenching) and hence the best energy transfer in the model compounds **1a** and **b**, which feature the closest cofactor arrangement. The most intense deazaflavin fluorescence, and consequently the least efficient energy transfer, was determined for the model compounds **3a/b** and **2a/b**, in which both cofactors are separated by two or four proline units, respectively. Although the proline spacer present only “semirigid” bridging units, the average distance between the two cofactors is clearly increased if proline units are inserted between the deazaflavin and the dimer. In the model compounds **3a/b** and **2a/b**, stacking of the two chromophores on top of each is not possible, which excludes that the observed fluorescence quenching is due to formation of a cofactor–cofactor complex. In summary, the data suggest that the energy flux from the deazaflavin to the reduced and deprotonated flavin is most efficient at small cofactor–cofactor distances and decreases in efficiency as the cofactor separation is increased.

Action Spectra and Investigation of the Splitting Reaction.

To firmly establish that the fluorescence reduction of the deazaflavins in the model compounds is caused by an intramolecular energy transfer to the FlH⁻ unit, action spectra (splitting rates depending on the irradiation wavelengths) of the model compounds were recorded. Previous measurements showed that deazaflavins alone are unable to initiate the splitting of cyclobutane pyrimidine dimers.²⁵ If, however, an energy transfer from the deazaflavin to the reduced and deprotonated flavin occurs, a significant shift in the action spectrum should be observed. With our model compounds, all action spectra were recorded in ethylene glycol, and the splitting rates were determined as described, in detail.³⁰ Briefly, the model compounds were dissolved, reduced with dithionite, and irradiated at various wavelengths between 360 and 470 nm. HPLC-analysis of the reaction solutions after certain irradiation time intervals allowed the determination of the conversion rate at each wavelength by quantification of the amount of starting material and product.

Three representative action spectra of the model compounds **5**, **4a**, and **4b** are depicted in Figure 2C. The reference compound **5**, which contains only a flavin cofactor and no deazaflavin, exhibits maximal absorption at 370 nm. This is also the wavelength at which maximal repair is observed. The model compound **4a** and all other series a model compounds, in contrast, show the most intense absorption around 390 and 410 nm due to the presence of the benzylated deazaflavin. In the action spectra of these model compounds, maximal repair is observed around 400 nm, which proves that the light that is absorbed by the deazaflavin chromophore is transferred to the reduced and deprotonated flavin unit, where it is used to drive the cleavage reaction. Model compound **4b** and all model compounds of series b exhibit maximal repair at 430 nm. This is, again, the wavelength at which the deprotonated deazaflavin absorbs most intensely. The result again shows that the light that is absorbed by the “quinoid” deazaflavin is used to drive the splitting reaction. The action spectra consequently support the hypothesis that both types of deazaflavins act in our model compounds solely as light-harvesting photoantennas. Absorption of light by the deazaflavin and subsequent energy transfer yields

(41) Eker, A. P. M.; Hessel, J. K. C.; Dekker, R. H. *Photochem. Photobiol.* **1986**, *44*, 197–205.

(42) Yasui, A.; Eker, A. P. M.; Yasuhira, S.; Yajima, H.; Kobayashi, T.; Takao, M.; Oikawa, A. *EMBO J.* **1994**, *13*, 6143–6151.

(43) Becker, H. G. O. *Einführung in die Photochemie*, 3. Auflage ed.; Deutscher Verlag der Wissenschaften: Berlin, 1991.

(44) Förster, T. *Discuss. Faraday Soc.* **1959**, *27*, 7–17.

an excited FlH^* chromophore, which initiates an electron transfer to the dimer lesion. All three action spectra are in full agreement with the $\text{dFl} \rightarrow \text{FlH}^-$ energy-transfer model.

Since the energy-transfer efficiency is maximal in the model compounds **1a** and **1b**, which possess the closest cofactor-cofactor arrangement, one would predict—based on our knowledge about the flavin-deazaflavin system—most efficient dimer splitting in these model systems.

To investigate this hypothesis, the splitting efficiencies of all model compounds were investigated upon irradiation with the wavelength at which maximal repair occurs. The model compounds of series a were irradiated at 400 nm, and the splitting reactions of all model compounds belonging to series b were investigated at 430 nm. The obtained splitting rates for the model compounds are depicted in Figure 4A for series a and in Figure 4B for series b. It is evident that all model compounds possess largely differing cleavage rates. The quantum yields for the dimer splitting were calculated from these rate data and the cofactor absorptions. The quantum yields are listed in Table 1, together with the estimated averaged cofactor distances, which were obtained from molecular modeling investigations. The obtained distance data were verified by short-time spectroscopic measurements.⁴⁵

The presentation of the repair rate data shows, in sharp contrast to our expectations, that the model compounds **1a** and **1b**, which possess the closest cofactor-cofactor distance and the most efficient energy transfer, are unable to perform an acceptable repair. Both compounds possess long half-life times for the splitting reaction of 78 (**1a**) and 32 min (**1b**), as extrapolated from the data shown in Figure 4. The reference compound **5**, in contrast, possesses a significantly shorter half-life time of $t_{1/2} = 18$ min at 366 nm (data not shown) and 32 min at 400 nm irradiation, despite the lack of a second deazaflavin cofactor. Only at 430 nm is this compound slower compared to **1b** because the flavin possess only negligible absorption at this wavelength. The deazaflavin consequently inhibits the repair process! During the irradiation of **1a** and **1b**, no products other than the expected cleavage compounds were detected. This excludes photodecomposition as a possible explanation for the observed very slow cleavage rates. Investigation of the whole model compound series showed that all the model compounds which possess the largest cofactor-cofactor distance cleave the dimer unit upon irradiation most efficient. Both model compounds (**2a** and **2b**), which possess four proline spacer, split the dimer lesions by a factor of 40 (!) faster than **1a** and **1b**. The model compounds **2a** and **2b** possess $t_{1/2}$ values of only 2 and 1 min, respectively. All model compounds which possess intermediate cofactor-cofactor distances feature intermediate half-life times. $t_{1/2}$ values of 13 and 8 min were measured for the model compounds **4a** and **4b**. The two proline-containing model compounds, **3a** and **3b**, require 9 and 3 min to reach the 50% cleavage level.

The quantum yields for the splitting reaction of all model compounds were determined by ferrioxalate actinometry.⁴⁶ In agreement with the slow dimer splitting, we measured very low quantum yields of approximately 1% for the model compounds **1a** and **1b**. These are the lowest values measured in the whole series. The model compounds **2a** and **2b**, which repair the dimer

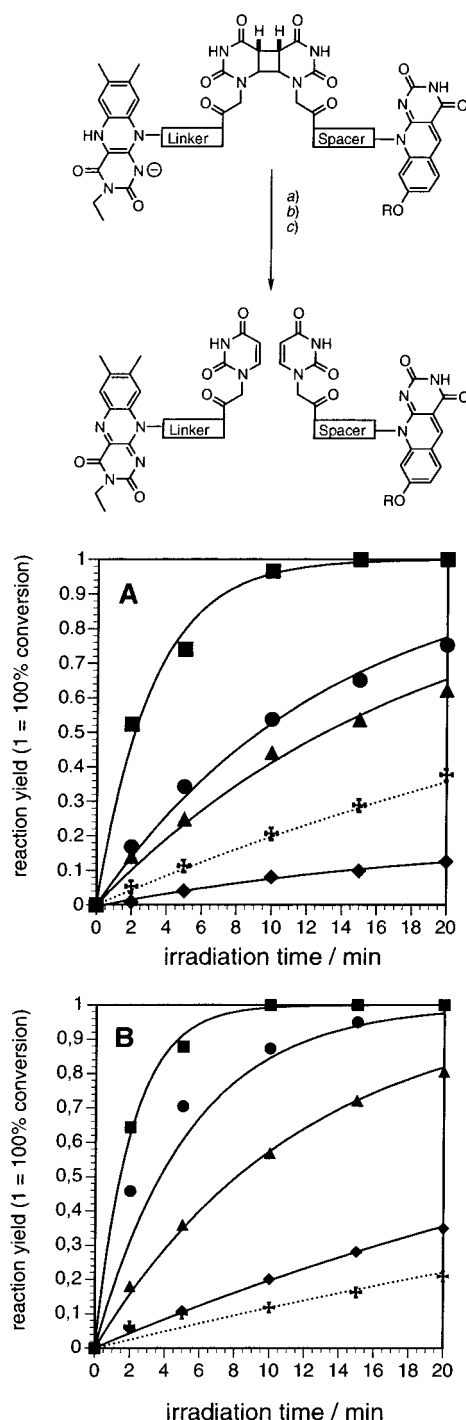


Figure 4. (A) Repair rates determined for the model compounds **1a**–**4a** in series a (**1a**, \blacklozenge ; **4a**, \blacktriangle ; **3a**, \bullet ; **2a**, \blacksquare ; **5**, \oplus). (B) Repair rates determined for the model compounds **1b**–**4b** in series b (**1b**, \blacklozenge ; **4b**, \blacktriangle ; **3b**, \bullet ; **2b**, \blacksquare ; **5**, \oplus). The model compounds were measured in ethylene glycol as the solvent and were reduced (flavin only) with sodium dithionite. The solutions were irradiated with monochromatic light at 400 (A) and 430 nm (B). The amount of photocleaved product versus the irradiation time was determined by reversed-phase HPLC as reported earlier in detail.³⁰ (a) Irradiation, (b) reoxidation, (c) HPLC analysis.

most efficiently and possess the largest cofactor-cofactor distance, show the best repair quantum yields of $\Phi \approx 10\%$. The model compounds **3a/b** and **4a/b** possess intermediate quantum yields, consistent with the observed rate data.

In summary, the cleavage data unequivocally show that the repair activity is strongly influenced by the distance between

(45) Michel-Beyerle, M. E.; Carell, T., unpublished results. The deazaflavin is also able to perform an energy transfer to the oxidized flavin. This energy transfer was investigated by short-time laser fluorescence spectroscopy. The distances between the cofactors were estimated from the fluorescence lifetimes according to the Förster theory.

(46) Hatchard, C. G.; Parker, C. A. *Proc. R. Soc. A* **1956**, *235*, 518–536.

Table 1. Repair Quantum Yields, Φ_{repair} ,^a of **1a–4a** (Series a) Measured upon Irradiation at 400 nm, of **1b–4b** (Series b) Measured upon Irradiation at 430 nm, and of the Reference Compound **5** Measured at 400 and 430 nm^b

model compound	flavin state	deazaflavin state	approximate Fl–dFl distance (Å)	$t_{1/2}$ (min)	Φ
2a	Fl _{red} H ⁻	dFl _{ox} -OBn	19	2	0.10
3a	Fl _{red} H ⁻	dFl _{ox} -OBn	16	9	0.03
4a	Fl _{red} H ⁻	dFl _{ox} -OBn	12	13	0.02
1a	Fl _{red} H ⁻	dFl _{ox} -OBn	7	78	0.005
5	Fl _{red} H ⁻	dFl _{ox} -OBn	—	32	0.08
2b	Fl _{red} H ⁻	dFl _{ox} -O ⁻	19	1	0.10
3b	Fl _{red} H ⁻	dFl _{ox} -O ⁻	16	3	0.06
4b	Fl _{red} H ⁻	dFl _{ox} -O ⁻	12	8	0.02
1b	Fl _{red} H ⁻	dFl _{ox} -O ⁻	7	32	0.01
5	Fl _{red} H ⁻	dFl _{ox} -O ⁻	—	50	0.08

^a Photon flux of the light source was determined by ferrioxalate actinometry. ^b $t_{1/2}$ is the half-life time for the cleavage of the model compounds. The average cofactor distance was determined on the basis of computer modeling (Macromodel, AMBER* force field). The distance estimates are supported by data from short-time fluorescence spectroscopic measurements.⁴⁵ Estimated error in $\Phi_{\text{Repair}} = \pm 20\%$. Estimated error for the average Fl–dFl distance = ± 2 Å.

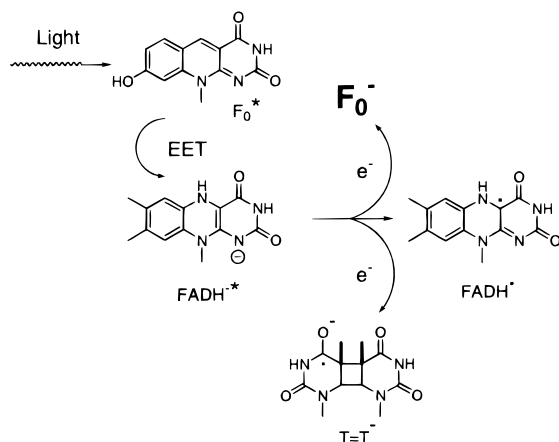


Figure 5. Schematic representation of the model of the electron-transfer possibilities between a FADH^{2*}, a deazaflavin (F₀), and a thymine dimer (T=T) after excitation of the FADH²⁻. EET = Excitation energy transfer.

the cofactors. Increasing flavin–deazaflavin distances yields decreasing half-life times for the splitting reaction. The cleavage data show that the presence of a deazaflavin cofactor in close proximity to the electron-donating FlH^{-*} inhibits the cleavage reaction. At larger cofactor–cofactor distances, the splitting rate increases, although the energy flux from the deazaflavin to the FlH⁻ is reduced.

This counterintuitive result shows that a large cofactor separation is required if efficient dimer splitting is desired. The results suggest that the deazaflavin cofactor can intercept the electron transfer from the flavin to the dimer lesion. At close cofactor distances, such as in **1a/1b**, this property fully inhibits the repair reaction. Due to the strong distance dependence of the inhibitory effect, we believe that the deazaflavin functions as an internal electron acceptor and induces a short-circuit electron transfer between the reduced flavin and the deazaflavin at short distances. If the deazaflavin is positioned too close to the reduced and deprotonated flavin, it functions as an alternative electron acceptor, as shown in Figure 5. This electron-transfer model is supported by all fluorescence and quantum yield data. In contrast to the through-space energy-transfer process, which is effective over relatively large distances (100 Å),^{44,47,48} through-bond electron-transfer reactions possess an e^{-r} distance

dependence and decrease more rapidly at larger distances.^{1,4,49} The increasing through-bond distances between the flavin and the deazaflavin cofactors in the model compounds **3a/b** and **2a/b**, which possess two or even four proline spacers,^{27,28} respectively, should affect the short-circuit intercofactor electron transfer more strongly than the beneficial energy transfer from the deazaflavin to the FlH⁻. This is indeed observed: the repair rate rises in both series of model compounds by a factor of approximately 50 from $t_{1/2} = 78$ min (**1a**) and $t_{1/2} = 32$ min (**1b**) to about 1–2 min in **2a** and **2b**, while at the same time, the energy-transfer efficiency shrinks to about one-quarter in **2a** and **2b** compared to that in **1a** and **1b** (Figure 3A,B). The electron-transfer model could also explain why all model compounds in series b are more “repair-active” compared to their counterparts in series a. In the models of series b, the deazaflavin is deprotonated and negatively charged, which should attenuate its electron-accepting properties. We measured almost maximal repair efficiency in series b already with compound **3b** (60% efficiency compared to **2b**). In series a, in contrast, compound **3a** is still a factor of 3 slower compared to **2a**. The electron-transfer model is also consistent with the available redox potentials. The light-excited, reduced, and deprotonated flavin possesses an estimated redox potential of -2.8 V.⁵⁰ The potential for the reduction of the dimer unit is approximately -2.2 V,⁵⁰ and the reduction potentials of the deazaflavins are likely to be between -0.8 and -1.5 V.⁵¹ An electron transfer from the light excited, reduced, and deprotonated flavin to the deazaflavin is, consequently, thermodynamically more favorable than that to the dimer unit.

Summary and Conclusion

These studies reveal that the repair activity in our model compounds critically depends on the cofactor–cofactor distance and the cofactors’ redox and protonation states. At large cofactor–cofactor distances, the deazaflavin functions exclusively as a photoantenna and channels light energy to the reduced flavin, where it is used to drive the electron transfer to the dimer unit. The dimer undergoes spontaneous cleavage as its radical anion. At shorter distances, the light-channeling process is more efficient, but the repair activity is strongly reduced. All our data, in combination with the available redox potentials, suggest a competitive light-induced electron transfer from the reduced flavin to the deazaflavin. This process represses the splitting reaction at close cofactor–cofactor distances. To achieve maximal repair efficiency, both cofactors have to be separated until this competitive process becomes negligible. It is very likely that photolyases faced the same problem and that they had to evolve strategies to circumvent the possibility of intrinsic electron transfer between the essential cofactors. From our data and based on the knowledge of DNA photolyase crystal structures, we argue that they may have solved this problem by tuning two main parameters: (1) The deazaflavin is deprotonated to attenuate its electron acceptor function. (2) The flavin and the deazaflavin distance is extended until the electron donation to the deazaflavin is efficiently suppressed. In addition, deazaflavin-containing photolyases

(47) Lankiewicz, L.; Malicka, J.; Wiszk, W. *Acta Biochim. Pol.* **1997**, *44*, 477–490.

(48) Van der Meer, B. W.; Coker, G., III; Chen, S.-Y. *Resonance Energy Transfer*; VCH Verlagsgesellschaft: Weinheim, 1994.

(49) Marcus, R. A.; Sutin, N. *Biochim. Biophys.* **1985**, *811*, 265–322.

(50) Scannel, M. P.; Fenick, D. J.; Yeh, S.-R.; Falvey, D. E. *J. Am. Chem. Soc.* **1997**, *119*, 1971–1977.

(51) van der Plas, H. C.; Link, P. A. *J. Org. Chem.* **1986**, *51*, 1602–1606.

feature, despite the large cofactor–cofactor distance, an excellent energy-transfer efficiency (98%). This transfer efficiency is far higher than that in our best compounds, **2a** and **2b**, which possess a random cofactor orientation. This suggests that photolyases also optimized the cofactors' orientations, to make the energy transfer most efficient even at the required large cofactor distance of 17 Å. Our data show that the large cofactor–cofactor distances observed in photolyases are an essential structural feature that will undoubtedly strongly determine their catalytic efficiency. The distance is not, as previously hypothesized,⁵² “not optimized during evolution”. Although the strict requirement for a large cofactor separation was shown with flavin- and deazaflavin-containing model compounds, we believe that similar reasons apply to the flavin–folate system in folate-containing type I photolyases. These types of photolyases also feature a surprisingly large cofactor–cofactor distance, and they possess additionally an unfavorable cofactor–cofactor orientation.

Experimental Part

General Methods. All materials were obtained from commercial suppliers and were used without further purification. Solvents of technical quality were distilled prior to use. The aqueous buffers were prepared using deionized water. For reactions under an inert gas atmosphere, nitrogen of standard quality was used. For analytical thin-layer chromatography, precoated silica gel plates (Merck 60-F254) were used. Staining of amino compounds was performed with ninhydrin. Flash chromatography was performed using silica gel (Merck, 0.040–0.063 mm) and silica gel-*H* (Fluka, 0.005–0.040 mm). Melting points are uncorrected and were determined on a Büchi Smp 20. IR spectra were recorded on a Perkin-Elmer 1600 FT-IR using KBr pellets or CHCl₃ solutions. UV spectra were recorded on a Varian Cary 5 UV–vis spectrophotometer in 1-cm quartz cuvettes. Fluorescence spectra were measured on a Spex 1680 0.22m double spectrometer with a bandwidth of 3.4 nm in 1-cm quartz cuvettes. NMR spectra were recorded on a Varian Gemini 200 (200 MHz (¹H), 50 MHz (¹³C)), a Varian Gemini 300 (300 MHz (¹H), 75 MHz (¹³C)), and a Bruker AM-500 (500 MHz (¹H), 125 MHz (¹³C)). The chemical shift (δ) is reported in ppm downfield from tetramethylsilane (TMS, $\delta = 0$ ppm). Alternatively, the resonances of residual solvent protons were used as the reference. EI mass spectra and FAB mass spectra were measured by the staff of the mass spectrometry facilities of the ETH Zurich on a Hitachi-Perkin-Elmer VG TRIBRID with 70-eV ionization energy (EI) and on a ZAB-2 SEQ with 3-nitrobenzyl alcohol as the matrix (FAB). MALDI-TOF spectra were measured on a Bruker Reflex spectrometer. ESI spectra were recorded on a Finnigan TSQ 7000. Elemental analyses were performed at the microanalysis laboratory of the ETH Zurich. HPLC chromatograms were obtained with a Knauer HPLC instrument (HPLC pumps 64, Knauer variable-wavelength UV detector, Knauer degasser) using HPLC grade solvents.

10-[2-(((*tert*-Butyl)oxy)carbonyl)amino)ethyl]-7,8-dimethyl-3-pentyl-3*H*,10*H*-benzo[*g*]pteridine-2,4-dione (18**).** 1-Bromopentane (588 mg, 3.89 mmol, 0.48 mL) was added with a syringe slowly to a suspension of the flavin compound **15** (500 mg, 1.30 mmol) and dry Cs₂CO₃ (0.6 g, 1.83 mmol) in DMF (50 mL, dried over 4-Å molecular sieves). The reaction mixture was stirred at room temperature for 3 h. The reaction mixture was diluted with CHCl₃ (200 mL) and washed three times with H₂O (3 × 80 mL). The organic phase was separated, dried with MgSO₄, filtered, and evaporated to dryness. The product **18** was obtained after column chromatography on silica gel-*H* (*d* = 3 cm, *l* = 18 cm) with CHCl₃/MeOH (20:1) as the eluent and recrystallization from MeOH/H₂O as yellow needles (140 mg, 24%). *R*_f(CHCl₃/MeOH, 20:1): 0.46. Mp: 228–230 °C. IR (KBr): 3329w, 2931w, 2867w, 1706m, 1691m, 1644s, 1583s, 1547s, 1450m, 1433m, 1366m, 1336m,

1289m, 1230m, 1206m, 1175m, 1072w, 1015w, 885w, 807w. ¹H NMR (400 MHz, (CD₃)₂SO): δ 0.88 (t, *J* = 6.7 Hz, 3 H), 1.22 (s, 9 H), 1.32 (m, 4 H), 1.58 (m, 2 H), 2.41 (s, 3 H), 2.50 (s, 3 H), 3.41 (q, *J* = 5.9 Hz, 2 H), 3.88 (t, *J* = 7.4 Hz, 2 H), 4.67 (t, *J* = 5.9 Hz, 2 H), 6.96 (t, *J* = 5.9 Hz, 1 H), 7.85 (s, 1 H), 7.93 (s, 1 H). ¹³C NMR (100 MHz, (CD₃)₂SO): δ 13.78, 18.68, 20.76, 21.85, 27.00, 27.93 (3C), 28.55, 36.95, 40.77, 44.00, 77.80, 116.16, 130.94, 131.41, 134.18, 135.72, 135.93, 146.43, 148.96, 154.63, 155.74, 159.35. MS (FAB): *m/z* 456 (100, [M + 1]⁺), 356 (53), 313 (71), 243 (36), 198 (28). Anal. Calcd for C₂₄H₃₃N₅O₄ + 0.5H₂O (464.57): C, 62.05; H, 7.38; N, 15.07. Found: C, 62.21; H, 7.23; N, 15.04.

10-(2-Aminoethyl)-7,8-dimethyl-3-pentyl-3*H*,10*H*-benzo[*g*]pteridine-2,4-dione, TFA Salt (7**).** A solution of the Boc-protected flavin **18** (180 mg, 0.40 mmol) in TFA/H₂O (95:5) (5 mL) was stirred at room temperature for 90 min. The reaction solution was evaporated to dryness in vacuo. The product **7** was filtered off after the addition of Et₂O. **7** was obtained as a yellow powder and used without further purification (180 mg, 97%). *R*_f(CHCl₃/MeOH/AcOH, 5:1:1): 0.38. Mp: 196–198 °C. IR (KBr): 3433w, 3100w, 3033w, 2958w, 2856w, 1689s, 1660s, 1584s, 1549s, 1461m, 1436m, 1411w, 1349w, 1254m, 1201m, 1133m, 1133m, 1020w, 798w, 722w. ¹H NMR (500 MHz, (CD₃)₂SO): δ 0.88 (t, *J* = 6.9 Hz, 3 H), 1.32 (m, 4 H), 1.59 (m, 2 H), 2.41 (s, 3 H), 2.51 (s, 3 H), 3.24 (t, *J* = 6.5 Hz, 2 H), 3.89 (t, *J* = 7.4 Hz, 2 H), 4.88 (t, *J* = 6.5 Hz, 2 H), 7.84 (s, 1 H), 7.97 (s, 1 H), 8.02 (br s, 2–3 H). ¹³C NMR (125 MHz, (CD₃)₂SO): δ 13.80, 18.70, 20.58, 21.85, 26.98, 28.54, 36.48, 40.84, 41.11, 115.63, 130.47, 131.26, 134.14, 136.04, 136.36, 146.98, 149.61, 154.66, 159.25. HRMS (FAB) for C₁₉H₂₆N₅O₂: (MH⁺) calcd 356.2086, found 356.2092.

***tert*-Butyl 2-[10-[2-(((*tert*-Butyl)oxy)carbonyl)amino)ethyl]-7,8-dimethyl-2,4-dioxo-3*H*,10*H*-benzo[*g*]pteridin-3-yl]acetate (**16**).** A suspension of the flavin **15** (1 g, 2.59 mmol), Cs₂CO₃ (1 g, 3.07 mmol), and *tert*-butyl bromoacetate (1.5 g, 7.69 mmol) in DMF (100 mL) was stirred for 5 h at room temperature. The reaction mixture was diluted with CHCl₃ (250 mL) and washed three times with H₂O (150 mL). The organic phase was separated, dried with MgSO₄, filtered, and concentrated in vacuo to dryness. The crude product **16** was precipitated through the addition of acetone/H₂O and filtered off. **16** was obtained after column chromatography on silica gel-60 (*d* = 3 cm, *l* = 18 cm, CHCl₃/MeOH, 15:1) and recrystallization from EtOAc/Ether as yellow needles (0.93 g, 75%). *R*_f(CHCl₃/MeOH, 10:1): 0.73. Mp: 198–200 °C. IR (CHCl₃): 3458w, 3007m, 3000m, 1742m, 1709s, 1661s, 1628w, 1584s, 1549s, 1504m, 1460m, 1369m, 1157s, 855w. ¹H NMR (400 MHz, (CD₃)₂SO): δ 1.22 (s, 9 H), 1.43 (s, 9 H), 2.42 (s, 3 H), 2.52 (s, 3 H), 3.45 (q, *J* = 5.9 Hz, 2 H), 4.54 (s, 2 H), 4.70 (t, *J* = 5.9 Hz, 2 H), 6.97 (t, *J* = 5.9 Hz, 1 H), 7.90 (s, 1 H), 7.97 (s, 1 H). ¹³C NMR (100 MHz, (CD₃)₂SO): δ 18.68, 20.83, 27.63 (3C), 27.90 (3C), 36.95, 42.90, 44.39, 77.84, 81.35, 116.34, 131.00, 131.69, 134.45, 135.36, 136.13, 147.03, 149.10, 154.12, 155.75, 159.18, 166.97. MS (FAB): *m/z* 500 (100, [M + 1]⁺), 388 (9), 344 (28), 198 (9). Anal. Calcd for C₂₅H₃₃N₅O₆ (499.57): C, 60.11; H, 6.66; N, 14.02. Found: C, 60.16; H, 6.48; N, 14.00.

2-[10-(2-Aminoethyl)-7,8-dimethyl-2,4-dioxo-3*H*,10*H*-benzo[*g*]pteridin-3-yl]acetic Acid, TFA Salt (17**).** A solution of **16** (0.8 g, 0.160 mmol) in TFA/H₂O (95:5) (20 mL) was stirred for 2 h at room temperature. The reaction mixture was subsequently evaporated to dryness, and the product was precipitated through the addition of Et₂O to the residual oil. The product was filtered off, washed with Et₂O, and dried under high vacuum. **17** (0.73 g, quantitative) was used in the next step without further purification. *R*_f(CHCl₃/MeOH/AcOH, 5:1:1): 0.45. Mp: 153–155 °C. IR (KBr): 3600–3200m, 3100–2700w, 1702m, 1661m, 1584m, 1548s, 1464w, 1352w, 1325w, 1247m, 1197m, 1136m, 1036w, 936w, 802w, 725w. ¹H NMR (500 MHz, (CD₃)₂SO): δ 2.43 (s, 3 H), 2.53 (s, 3 H), 3.27 (m, 2 H), 4.59 (s, 2 H), 4.91 (t, *J* = 6.4 Hz, 2 H), 7.89 (s, 1 H), 8.01 (s, 1 H), 8.05 (br s, 2–3 H), 11.5–13.5 (br s, 1 H). ¹³C NMR (125 MHz, (CD₃)₂SO): δ 18.70, 20.63, 39.00, 41.48, 42.36, 115.77, 130.78, 131.36, 134.44, 135.85, 136.39, 147.60, 149.80, 154.23, 159.08, 169.21. HRMS (FAB) for C₁₈H₁₈N₅O₆F₃ (457.37): (MH⁺ – CF₃COO) calcd 344.1359, found 344.1359.

2-[10-[2-(((Fluoren-9-yl)methoxy)carbonyl)amino)ethyl]-7,8-dimethyl-2,4-dioxo-3*H*,10*H*-benzo[*g*]pteridin-3-yl]acetic Acid (9**).** A suspension of the flavin amino acid **17** (250 mg, 0.55 mmol) in aqueous

(52) Park et al. proposed, for the folate-containing type-I photolyases, that the energy transfer within photolyases is not rate limiting. In this case, we would expect identical repair rates for all prepared model compounds, independent from the flavin–deazaflavin distance. This is clearly not observed. All compounds feature largely different repair efficiencies.

K₂CO₃ solution (9%, 10 mL) was stirred and cooled to 0 °C. Then, Fmoc-OSu (300 mg, 0.89 mmol), dissolved in 2 mL of DMF, was added. The solution was stirred for 90 min and allowed to warm to room temperature during this time. The reaction mixture was diluted with H₂O (250 mL) and acidified (pH = 3.5) through the addition of a 10% citric acid solution (100 mL). This solution was extracted three times with CHCl₃ (3 × 300 mL). The combined organic phases were separated, dried with MgSO₄, filtered, and concentrated in vacuo to dryness. Et₂O was added to the residual oil, and the reaction product was filtered off (**9**, 250 mg, 80%). *R*_f (CHCl₃/MeOH/AcOH, 5:1:1): 0.80. Mp: 179–181 °C. IR (KBr): 3600–3200m, 3056w, 2956w, 1711s, 1661s, 1583s, 1547s, 1450m, 1411w, 1350w, 1322w, 1261m, 1231m, 1206m, 1011w, 761w, 742w. ¹H NMR (400 MHz, (CD₃)₂SO): δ 2.29 (s, 3 H), 2.33 (s, 3 H), 3.51 (q, *J* = 5.9 Hz, 2 H), 4.05 (t, *J* = 7.0 Hz, 1 H), 4.21 (d, *J* = 7.0 Hz, 2 H), 4.53 (s, 2 H), 4.73 (t, *J* = 5.9 Hz, 2 H), 7.38–7.95 (m, 11 H), 11.5–13.5 (br s, 1 H). ¹³C NMR (100 MHz, (CD₃)₂SO): δ 18.57, 20.66, 37.06, 42.21, 43.62, 46.49, 65.63, 115.92, 119.98 (2C), 124.89 (2C), 126.91 (2C), 127.50 (2C), 130.99, 131.53, 134.36, 135.46, 136.06, 140.56 (2C), 143.66 (2C), 146.98, 149.10, 154.13, 156.41, 159.14, 169.23. HRMS (FAB) for C₃₁H₂₇N₅O₆: (MH⁺) calcd 566.2040, found 566.2065.

6-([2-((tert-Butyl)oxy)carbonyl]amino)ethyl]amino]-1H,3H-pyrimidine-2,4-dione (21). The mono-Boc-protected ethylenediamine **20**³³ (6.5 g, 41 mmol, 1.5 equiv) was added to a solution of 6-chlorouracil **19** (4 g, 27 mmol) in *n*-butanol (100 mL). This solution was heated for 4 h at reflux. The solution was cooled to room temperature, and the *n*-butanol was distilled off in vacuo. The residual material was dissolved in boiling water and then stored at 4 °C for 12 h. The colorless precipitate was filtered off and was once more recrystallized from water. The product **21** was obtained as a colorless microcrystalline powder (4.8 g, 65%). *R*_f (CHCl₃/MeOH, 10:1): 0.18. Mp: 221–223 °C. IR (KBr): 3310s, 3222s, 3100m, 2978m, 1726s, 1683s, 1596s, 1539s, 1449m, 1389m, 1364m, 1333m, 1277m, 1244m, 1223m, 1170m, 1106w, 1039w, 1017w, 987w, 964w, 829w, 806w, 767w, 548m. ¹H NMR (400 MHz, (CD₃)₂SO): δ 1.38 (s, 9 H), 3.05 (m, 4 H), 4.48 (s, 1 H), 6.08 (br s, 1 H), 6.89 (br s, 1 H), 9.98 (br s, 1 H), 10.12 (br s, 1 H). ¹³C NMR (100 MHz, (CD₃)₂SO): δ 28.17 (3C), 38.81, 41.09, 72.54, 77.81, 150.80, 154.08, 155.74, 164.24. MS (FAB): *m/z* 271 (96, [M + 1]⁺), 215 (22), 171 (31). Anal. Calcd for C₁₁H₁₈N₄O₄ (270.29): C, 48.88; H, 6.71; N, 20.73. Found: C, 48.98; H, 6.83; N, 20.70.

8-Benzyloxy-10-[2-((tert-butyl)oxy)carbonyl]amino)ethyl]-5-carba-3H,10H-benzog[*g*]pteridine-2,4-dione (22). A solution of 2,4-(dibenzyloxy)benzaldehyde (**23**) (2.1 g, 6.6 mmol) and the uracil derivative **21** (1 g, 3.7 mmol) in DMF (50 mL) was stirred for 20 h at 120 °C. The reaction solution was cooled to 4 °C, and the precipitated yellow reaction product **22** was isolated by filtration. The product was washed with Et₂O and was recrystallized twice from MeOH. **22** was obtained as a yellow, microcrystalline powder (0.9 g, 52%). *R*_f (CHCl₃/MeOH, 10:1): 0.41. Mp: 183–185 °C. IR (KBr): 3419m, 3133w, 2967w, 2811w, 1699s, 1661m, 1603s, 1561m, 1527s, 1492m, 1456m, 1405m, 1367m, 1242s, 1188m, 1188m, 1167m, 1144m, 983w, 796w, 579w. ¹H NMR (500 MHz, (CD₃)₂SO): δ 1.28 (s, 9 H), 3.36 (q, *J* = 6.5 Hz, 2 H), 4.67 (br s, 2 H), 5.41 (s, 2 H), 7.23 (m, 2 H), 7.38 (m, 1 H), 7.44 (m, 2 H), 7.53 (d, *J* = 7.1 Hz, 2 H), 7.71 (s, 1 H), 8.10 (d, *J* = 9.0 Hz, 1 H), 8.90 (s, 1 H), 10.97 (s, 1 H). ¹³C NMR (125 MHz, (CD₃)₂SO): δ 27.97 (3C), 36.81, 44.18, 70.34, 77.99, 99.91, 111.87, 114.85, 115.90, 127.91 (2C), 128.20, 128.51 (2C), 133.46, 135.89, 141.19, 142.87, 156.06, 156.50, 157.67, 162.24, 164.26. MS (FAB): *m/z* 463 (100, [M + 1]⁺), 389 (8), 363 (21). Anal. Calcd for C₂₅H₂₆N₄O₅ + H₂O (480.53): C, 62.49; H, 5.87; N, 11.66. Found: C, 62.39; H, 5.87; N, 11.66.

8-Benzyloxy-10-[2-((tert-butyl)oxy)carbonyl]amino)ethyl]-3-pentyl-5-carba-3H,10H-benzog[*g*]pteridine-2,4-dione (24). 1-Bromopentane (0.4 mL, 3.31 mmol) was added dropwise to a suspension of the deazaflavin **22** (0.5 g, 1.08 mmol) and dry Cs₂CO₃ (0.5 g, 1.53 mmol) in dry DMF (50 mL, dried over molecular sieves (4 Å)) at 60 °C. The reaction mixture was stirred for 2 h at this temperature. The reaction mixture was diluted with CHCl₃ (200 mL), and the organic phase was washed three times with H₂O (3 × 100 mL). The organic phase was separated, dried with MgSO₄, filtered, and concentrated in

vacuo. The solid material was recrystallized from CHCl₃/MeOH. The product **24** was obtained as yellow needles (0.4 g, 70%). *R*_f (CHCl₃/MeOH, 20:1): 0.67. Mp: 216–217 °C. IR (KBr): 3434m, 3044w, 2932w, 2867w, 1702m, 1638s, 1607s, 1537s, 1500m, 1457m, 1411w, 1367w, 1236s, 1167m, 1126w, 1006w, 956w, 798w. ¹H NMR (500 MHz, CDCl₃): δ 0.90 (t, *J* = 7.1 Hz, 3 H), 1.37 (m, 4 H), 1.46 (s, 9 H), 1.70 (m, 2 H), 3.55 (m, 2 H), 4.05 (t, *J* = 7.6 Hz, 2 H), 4.82 (br s, 2 H), 5.09 (t, *J* = 6.0 Hz, 1 H), 5.46 (s, 2 H), 7.13 (dd, *J* = 2.1 Hz, *J* = 8.8 Hz, 1 H), 7.36 (t, *J* = 7.2 Hz, 1 H), 7.42 (t, *J* = 7.2 Hz, 2 H), 7.53 (d, *J* = 7.2 Hz, 2 H), 7.77 (d, *J* = 8.8 Hz, 1 H), 7.93 (s, 1 H), 8.77 (s, 1 H). ¹³C NMR (125 MHz, CDCl₃): δ 14.03, 22.51, 27.63, 28.38 (3C), 29.21, 37.29, 41.35, 43.85, 71.10, 80.11, 99.39, 111.96, 116.23, 116.67, 127.68 (2C), 128.39, 128.72 (2C), 132.94, 135.87, 142.15, 143.27, 156.49, 156.69, 157.26, 162.17, 165.43. MS (FAB): *m/z* 533 (100, [M + 1]⁺), 460 (13), 433 (14), 390 (11). Anal. Calcd for C₃₀H₃₆N₄O₅ (532.64): C, 67.65; H, 6.81; N, 10.52. Found: C, 67.46; H, 6.73; N, 10.45.

10-(2-Aminoethyl)-8-benzyloxy-3-pentyl-5-carba-3H,10H-benzog[*g*]pteridine-2,4-dione, TFA Salt (10). A solution of the Boc-protected deazaflavin derivative **24** (300 mg, 0.56 mmol) in TFA/H₂O (95:5) was stirred for 2 h at room temperature. The reaction mixture was concentrated in vacuo, and the product **10** was crystallized through the addition of Et₂O to the residual oil. Compound **10** was filtered off and was obtained as the yellow trifluoroacetic acid salt (300 mg, 97%). *R*_f (CHCl₃/MeOH/HOAc, 5:1:1): 0.72. Mp: 241–243 °C. IR (KBr): 3426m, 3033w, 2944w, 1703m, 1606s, 1535s, 1500w, 1461w, 1417w, 1372w, 1254m, 1189m, 1150w, 994w, 739w. ¹H NMR (500 MHz, (CD₃)₂SO): δ 0.86 (t, *J* = 7.0 Hz, 3 H), 1.30 (m, 4 H), 1.56 (m, 2 H), 3.20 (m, 2 H), 3.86 (t, *J* = 7.4 Hz, 2 H), 4.90 (t, *J* = 6.3 Hz, 2 H), 5.38 (s, 2 H), 7.33 (dd, *J* = 1.9 Hz, *J* = 8.9 Hz, 1 H), 7.37–7.45 (m, 4 H), 7.53 (d, *J* = 7.2 Hz, 2 H), 7.98 (br s, 3 H), 8.19 (d, *J* = 8.9 Hz, 1 H), 8.97 (s, 1 H). ¹³C NMR (125 MHz, (CD₃)₂SO): δ 13.82, 21.84, 27.08, 28.59, 36.41, 40.18, 41.47, 70.53, 100.33, 111.62, 114.03, 116.33, 128.29 (2C), 128.38, 128.59 (2C), 134.21, 135.78, 142.03, 142.37, 155.65, 156.80, 161.43, 164.62. HRMS (FAB) for C₂₅H₂₈N₄O₃: (MH⁺) calcd 433.22397, found 433.2247.

tert-Butyl 2-([10-[2-((tert-butyl)oxy)carbonyl]amino)ethyl]-8-benzyloxy-2,4-dioxo-5-carba-3H,10H-benzog[*g*]pteridin-3-yl]-acetate (25). *tert*-Butyl bromoacetate (1.1 mL, 7.3 mmol) was added dropwise to a suspension of the deazaflavin **22** (1 g, 2.2 mmol) and dry Cs₂CO₃ (1 g, 3.06 mmol) in DMF (50 mL, dried over molecular sieves (4 Å)) at 60 °C. The reaction mixture was stirred for 5 h at 60 °C. The reaction mixture was subsequently diluted with CHCl₃ (200 mL), and the organic phase was washed three times with H₂O (3 × 100 mL). The organic phase was separated, dried with MgSO₄, filtered, and concentrated in vacuo. The residual material was subjected to column chromatography on silica gel-60 (*d* = 3 cm, *l* = 18 cm) with CHCl₃/MeOH (20:1) as the eluent. The product **25** was recrystallized from MeOH and obtained as yellow needles (0.62 g, 49%). *R*_f (CHCl₃/MeOH, 20:1): 0.74. Mp: 219–221 °C. IR (KBr): 3423m, 3044w, 2978w, 2933w, 1735m, 1691m, 1640s, 1609s, 1567m, 1537s, 1498s, 1456m, 1412m, 1370m, 1322w, 1289w, 1244s, 1189m, 1157m, 1039w, 990w, 937w, 828w, 796w. ¹H NMR (500 MHz, CDCl₃): δ 1.47 (s, 9 H), 1.48 (s, 9 H), 3.55 (q, *J* = 7.3 Hz, 2 H), 4.73 (s, 2 H), 4.83 (br s, 1 H), 5.06 (t, *J* = 6.1 Hz, 1 H), 5.47 (s, 2 H), 7.15 (dd, *J* = 2.2 Hz, *J* = 8.8 Hz, 1 H), 7.37 (m, 1 H), 7.42 (m, 2 H), 7.54 (d, *J* = 7.3 Hz, 2 H), 7.77 (d, *J* = 8.8 Hz, 2 H), 7.98 (d, *J* = 1.5 Hz, 1 H), 8.80 (s, 1 H). ¹³C NMR (125 MHz, CDCl₃): δ 28.10 (3C), 28.38 (3C), 37.26, 42.99, 44.05, 71.17, 77.29, 80.16, 81.97, 99.44, 111.56, 116.25, 116.96, 127.70 (2C), 128.41, 128.73 (2C), 133.02, 135.83, 142.56, 143.46, 156.71, 156.73, 161.98, 165.66, 167.42. MS (FAB): *m/z* 577 (100, [M + 1]⁺), 521 (9), 503 (10), 434 (21), 421 (44). Anal. Calcd for C₃₁H₃₆N₄O₇ (576.65): C, 64.57; H, 6.29; N, 9.72. Found: C, 64.42; H, 6.25; N, 9.65.

tert-Butyl 2-([10-[2-((tert-butyl)oxy)carbonyl]amino)ethyl]-8-hydroxy-2,4-dioxo-5-carba-3H,10H-benzog[*g*]pteridin-3-yl]-acetate (31). The benzylated compound **25** (300 mg, 0.52 mmol) was dissolved at room temperature in acetic acid (30 mL). A suspension of Pd/BaSO₄ (15 mg) in acetic acid (3 mL) was added, and the reaction mixture was stirred in an H₂ atmosphere for 20 h. The reaction mixture was filtered through Celite, and the solution was evaporated in vacuo.

Diethyl ether was added to the residual oil to precipitate the product **31**, which was filtered off and dried in vacuo (250 mg, quantitative). Mp: 152–154 °C. IR (KBr): 3426m, 2978w, 2922w, 1744m, 1701m, 1639s, 1606s, 1578m, 1534m, 1511s, 1472m, 1394m, 1367m, 1267m, 1228m, 1161s, 1039w, 967w, 939w, 856w, 806w, 794w. ¹H NMR (400 MHz, (CD₃)₂SO): δ 1.28 (s, 9 H), 1.42 (s, 9 H), 3.38 (q, *J* = 6.0 Hz, 2 H), 3.40 (br s, 1 H), 4.50 (s, 2 H), 4.63 (t, *J* = 6.0 Hz, 2 H), 7.04–7.09 (m, 2 H), 7.26 (s, 1 H), 8.04 (d, *J* = 8.9 Hz, 1 H), 8.90 (s, 1 H). ¹³C NMR (100 MHz, (CD₃)₂SO): δ 27.59 (3C), 27.96 (3C), 36.99, 42.23, 44.08, 77.75, 81.04, 100.96, 109.28, 115.27, 115.53, 134.07, 142.26, 143.55, 155.22, 155.76, 156.15, 161.46, 165.48, 167.27. HRMS (FAB) for C₂₄H₃₀N₄O₇ (486.53): (*M* + 1⁺) calcd 487.2193, found 487.2192.

[10-(2-Aminoethyl)-8-benzyloxy-2,4-dioxo-5-carba-3H,10H-benzog[pteridin-3-yl]acetic Acid, TFA Salt (26). A solution of **25** (680 mg, 1.2 mmol) in 15 mL of TFA/H₂O (95:5) was stirred at room temperature for 3 h. The reaction mixture was concentrated in vacuo, and Et₂O was added to the residual oil. **26** was filtered off, washed with Et₂O, and dried under high vacuum. **26** was obtained as a yellow powder (640 mg, quantitative). *R_f* (CHCl₃/MeOH/HOAc, 5:1:1): 0.09. Mp: 251–253 °C. IR (KBr): 3422m, 3400–2300m, 1689m, 1603s, 1534s, 1494m, 1467m, 1416w, 1367w, 1317w, 1260m, 1194m, 1172m, 1133m, 1033w, 983w, 944w, 833w, 794w, 721w. ¹H NMR (400 MHz, (CD₃)₂SO): δ 3.26 (t, *J* = 6.1 Hz, 2 H), 4.56 (s, 2 H), 4.94 (br s, 2 H), 5.40 (s, 2 H), 7.34–7.47 (m, 5 H), 7.54 (d, 2 H), 8.10 (br s, 3 H), 8.21 (d, *J* = 8.8 Hz, 1 H), 9.00 (s, 1 H), 11.80–13.50 (br s, 1 H). ¹³C NMR (100 MHz, (CD₃)₂SO): δ 36.22, 41.75, 41.80, 70.20, 100.32, 111.12, 114.40, 116.44, 128.33 (2C), 128.40, 128.61 (2C), 134.35, 135.77, 142.33, 142.87, 155.30, 156.90, 161.28, 164.91, 169.52. HRMS (FAB) for C₂₄H₂₁N₄O₇F₃ (534.45): (*M*⁺ – CF₃COO) calcd 421.1512, found 421.1513.

2-[[10-[2-((Fluoren-9-yl)methoxy)carbonyl]amino)ethyl]-8-benzyloxy-2,4-dioxo-5-carba-3H,10H-benzog[pteridin-3-yl]acetic Acid (11). The deazaflavin amino acid **26** (250 mg, 0.47 mmol) was suspended in aqueous K₂CO₃ solution (9%, 15 mL) and cooled to 4 °C. A solution of Fmoc-OSu (300 mg, 0.89 mmol) in DMF (1 mL) was slowly added. The suspension was stirred for another 90 min, and the reaction mixture was allowed to warm to room temperature during this time. The reaction mixture was diluted with water (200 mL) and acidified (pH = 3.5) through the addition of an aqueous citric acid solution (10%, 100 mL). The mixture was extracted two times with CHCl₃. The combined organic phases were dried with MgSO₄, filtered, and concentrated in vacuo to dryness. The product **11** was dissolved in a small amount of CHCl₃ and precipitated through the addition of Et₂O. **11** was filtered off and dried under high vacuum (**11**, 220 mg, 73%). *R_f* (CHCl₃/MeOH/AcOH, 5:1:1): 0.92. Mp: 202–204 °C. IR (KBr): 3600–2500m, 3398m, 3333m, 3038w, 2952w, 1703s, 1605s, 1535s, 1490m, 1466m, 1417w, 1375w, 1254s, 1202m, 1152w, 996w, 792w, 742w. ¹H NMR (400 MHz, (CD₃)₂SO): δ 3.46 (q, *J* = 6.0 Hz, 2 H), 4.15 (t, *J* = 7.0 Hz, 1 H), 4.27 (d, *J* = 7.0 Hz, 2 H), 4.51 (s, 2 H), 4.74 (br s, 2 H), 5.30 (s, 2 H), 7.21 (dd, *J* = 2.0 Hz, *J* = 8.9 Hz, 1 H), 7.27 (t, *J* = 7.5 Hz, 2 H), 7.35–7.43 (m, 8 H), 7.55 (d, *J* = 7.5 Hz, 2 H), 7.70 (t, *J* = 6.0 Hz, 1 H), 7.86 (d, *J* = 7.5 Hz, 2 H), 8.15 (d, *J* = 9.0 Hz, 1 H), 8.99 (s, 1 H), 12.69 (br s, 1 H). ¹³C NMR (100 MHz, (CD₃)₂SO): δ 37.09, 41.73, 43.66, 46.61, 65.71, 70.33, 99.80, 110.89, 115.05, 116.22, 120.06 (2C), 124.99 (2C), 126.99 (2C), 127.56 (2C), 128.01 (2C), 128.24, 128.50 (2C), 133.79, 135.70, 140.66 (2C), 142.49, 142.95, 143.73 (2C), 155.27, 156.28, 156.72, 161.34, 164.57, 169.58. MS (FAB) for C₃₇H₃₀N₄O₇ (642.67): 643 (100, [*M* + 1]⁺), 460 (13). HRMS (FAB) for C₃₇H₃₀N₄O₇: (*MH*⁺) calcd 643.2193, found 643.2201.

Solid-Phase Synthesis of the Peptides 13 and 14. First, 2.2 g of a NovaBiochem Rink-Amide MBHA resin (0.62 mmol amine/g) was suspended in DMF (10 mL) and shaken for 2 h. The resin was shaken with 20% piperidine in DMF (10 mL) for 15 min and washed three times with DMF (5 mL). After a positive Kaiser test, the resin was washed another three times with NMP (5 mL). The Fmoc-protected amino acid **11** (1.10 g, 1.71 mmol) was dissolved in NMP and shaken together with HOBt (0.52 g, 3.42 mmol) and TBTU (1.10 g, 3.42 mmol) for 10 min. This mixture was added to the resin, and the slurry was shaken after the addition of diisopropylethylamine (DIEA) (1.91 mL,

11.16 mmol) for 48 h. The solution was filtered off, and the resin was washed three times for 3 min with NMP (5 mL) and three times for 3 min with DMF. After a negative Kaiser test, the resin was shaken with 20% piperidine in DMF (10 mL) for 15 min and washed three times with DMF (5 mL). Fmoc-protected proline (1.38 g, 4.09 mmol) was dissolved in NMP and shaken together with HOBt (0.73 g, 4.77 mmol) and TBTU (1.53 g, 4.77 mmol) for 5 min. This solution and DIEA (2.1 mL, 12.27 mmol) were added to the resin, and the slurry was shaken for 3 h. The solution was filtered off, and the resin was washed three times for 3 min with NMP (5 mL) and three times for 3 min with DMF. After a negative Kaiser test, the resin was shaken with 20% piperidine in DMF (10 mL) for 15 min and washed three times with DMF (5 mL). The coupling of the proline was repeated either once or three times for the synthesis of **13** and **14**, respectively. The resin was finally washed three times with DMF (5 mL), seven times with CH₂Cl₂ (10 mL), three times with MeOH (10 mL), and three times with Et₂O (10 mL). The resin was dried and shaken together with 15 mL of a solution of TFA (95%), H₂O (2.5%), and triisobutylsilane (TIS) (2.5%) for 1 h. The solution was filtered off and evaporated in vacuo. The peptides were precipitated through the addition of Et₂O. The crude peptides were purified by reversed-phase HPLC (RP18-column with a H₂O(1% TFA)/CH₃CN gradient (100% water to 100% acetonitrile over 100 min). Yields: **13**, 270 mg, 49%; **14**, 550 mg, 50%.

Data for 13. Mp: 110–112 °C. IR (KBr): 3600–2500m, 3400m, 3200m, 3067m, 2956m, 1678s, 1650s, 1604s, 1567m, 1535s, 1494m, 1461m, 1417m, 1372m, 1254s, 1198s, 1139m, 1026w, 994w, 933w, 833w, 795w, 721w, 700w. ¹H NMR (400 MHz, (CD₃)₂SO): δ 1.60–1.95 (m, 6 H), 2.08 (m, 1 H), 2.26 (m, 1 H), 3.05–3.30 (m, 2 H), 3.30–3.75 (m, 4 H), 4.31 (m, 1 H), 4.44 (m, 1 H), 4.45 (s, 2 H), 4.70 (m, 2 H), 5.42 (s, 2 H), 7.06 (s, 1 H), 7.26 (dd, *J* = 2.0 Hz, *J* = 8.9 Hz, 1 H), 7.38–7.56 (m, 6 H), 8.15 (d, *J* = 9.0 Hz, 1 H), 8.48 (br s, 1 H), 8.52 (t, *J* = 5.8 Hz, 1 H), 8.95 (s, 1 H), 9.50 (br s, 1 H). ¹³C NMR (100 MHz, (CD₃)₂SO): δ 23.36, 24.42, 27.65, 29.11, 35.46, 42.65, 42.97, 45.59, 46.69, 58.28, 59.84, 70.42, 99.78, 111.28, 115.13, 116.03, 128.26 (2C), 128.32, 128.54 (2C), 133.72, 135.81, 142.04, 142.58, 155.54, 156.16, 161.44, 164.52, 166.59, 168.88, 172.06. HRMS (FAB) for C₃₂H₃₅N₇O₆: (*MH*⁺) calcd 614.2727, found 614.2724.

Data for 14. Mp: 186–188 °C. IR (KBr): 3600–3000m, 3430m, 2967w, 2878w, 1678s, 1644s, 1605s, 1561w, 1535s, 1489w, 1455m, 1411m, 1367w, 1311w, 1252m, 1191m, 1161m, 1133m, 1022w, 928w, 833w, 794w. ¹H NMR (500 MHz, (CD₃)₂SO): δ 1.60–2.45 (m, 16 H), 3.05–3.70 (m, 10 H), 4.10–4.60 (m, 4 H), 4.44 (s, 2 H), 4.70 (m, 2 H), 5.44 (s, 2 H), 7.04 (s, 1 H), 7.25 (dd, *J* = 2.0 Hz, *J* = 8.8 Hz, 1 H), 7.37–7.55 (m, 6 H), 8.16 (d, *J* = 9.0 Hz, 1 H), 8.32 (t, *J* = 5.8 Hz, 1 H), 8.44 (br s, 1 H), 8.96 (s, 1 H), 9.39 (br s, 1 H). ¹³C NMR (125 MHz, (CD₃)₂SO): δ 23.42, 24.14, 24.26, 24.40, 27.38, 27.58, 28.92, 30.67, 35.68, 42.65, 43.09, 45.74, 46.35, 46.54, 46.61, 57.46, 57.82, 58.17, 59.40, 70.35, 99.78, 111.28, 115.24, 116.01, 128.24 (2C), 128.46, 128.49 (2C), 133.62, 135.85, 142.00, 142.66, 155.51, 156.17, 161.45, 164.51, 165.98, 168.56, 168.85, 172.86. MS (FAB) for C₄₂H₄₉N₉O₈: *m/z* 831 (16, [*M* + Na]⁺), 809 (100, [*M* + 1]⁺), 616 (4).

Flavin–Deazaflavin Peptide 27. The Fmoc-protected flavin amino acid **9** (285 mg, 0.50 mmol) was stirred together with BOP (1.00 g, 2.27 mmol) in DMF (30 mL) for 10 min. The deazaflavin **10** (275 mg, 0.50 mmol) was dissolved in 5 mL of DMF and added. Twenty drops of NEt₃ were added, and the reaction mixture was stirred for 90 min at room temperature. The reaction solution was diluted with water (100 mL) and extracted three times with CHCl₃. The combined organic phases were dried with MgSO₄, filtered, and concentrated in vacuo. The product **27** was dissolved in a small amount of CHCl₃ and precipitated with Et₂O. **27** was obtained after column chromatography on silica gel 60 (*d* = 3 cm, *l* = 18 cm) with CHCl₃/MeOH (20:1) as an orange-yellow powder (160 mg, 33%). *R_f* (CHCl₃/MeOH, 10:1): 0.58. Mp: 182–184 °C. IR (KBr): 3429m, 2950w, 2933w, 2856w, 1706m, 1639m, 1607s, 1578m, 1541s, 1456m, 1406w, 1250m, 1228m, 1022w, 739w. ¹H NMR (500 MHz, (CD₃)₂SO): 0.85 (t, *J* = 7.1 Hz, 3 H), 1.28 (m, 4 H), 1.53 (m, 2 H), 2.33 (s, 3 H), 2.38 (s, 3 H), 3.45 (m, 4 H), 3.83 (t, *J* = 7.4 Hz, 2 H), 4.08 (t, *J* = 6.9 Hz, 2 H), 4.24 (d, *J* = 6.9 Hz, 2 H), 4.45 (s, 2 H), 4.60 (m, 2 H), 4.72 (m, 2 H), 5.36 (s, 2 H), 7.21 (dd, *J* = 2.0 Hz, *J* = 8.9 Hz, 1 H), 7.26 (t, *J* = 7.4 Hz, 2 H), 7.27 (t, *J* = 7.4 Hz, 1 H), 7.33 (t, *J* = 7.4 Hz, 2 H), 7.39 (t, *J* =

7.4 Hz, 2 H), 7.46 (d, $J = 7.0$ Hz, 2 H), 7.54 (d, $J = 7.4$ Hz, 2 H), 7.73 (s, 1 H), 7.85 (d, $J = 7.4$ Hz, 2 H), 7.86 (s, 1 H), 7.94 (s, 1 H), 8.12 (d, $J = 8.9$ Hz, 1 H), 8.61 (t, $J = 5.8$ Hz, 1 H), 8.91 (s, 1 H). ^{13}C NMR (125 MHz, $(\text{CD}_3)_2\text{SO}$): δ 13.76, 18.61, 20.67, 21.78, 26.99, 28.55, 35.30, 37.10, 40.07, 42.91, 43.39, 43.68, 46.51, 65.59, 70.25, 99.44, 111.20, 115.18, 115.96, 119.96 (2C), 124.89 (2C), 126.88 (2C), 127.48 (2C), 127.73, 128.08 (2C), 128.16, 128.35 (2C), 130.98, 131.13, 133.51, 134.09, 135.75, 135.99, 136.06, 140.56 (2C), 141.91, 142.53, 143.66 (2C), 146.83, 149.03, 154.31, 155.60, 155.86, 156.41, 159.38, 161.38, 164.46, 168.28. HRMS (FAB) for $\text{C}_{56}\text{H}_{53}\text{N}_9\text{O}_8$: (M^+) calcd 980.4095, found 980.4092.

Model Compound 4a. BOP (300 mg, 0.646 mmol) was added to a solution of the *cis-syn*-biscarboxymethyluracil dimer **6** (100 mg, 0.30 mmol) in DMF (5 mL). This solution was stirred for 10 min at room temperature. A solution of the aminoethyl flavin **7** (150 mg, 0.32 mmol) in DMF (3 mL) and ca. 15 drops of NEt_3 were added. This solution was stirred for 30 min at room temperature. An excess of the aminoethyl-substituted deazaflavin **10** (230 mg, 0.42 mmol) dissolved in DMF (3 mL) was added, and the reaction mixture was stirred for another 30 min at room temperature. The reaction mixture was diluted with CHCl_3 (100 mL) and washed three times with H_2O (3×100 mL). The organic phase was dried with MgSO_4 , filtered, and concentrated in vacuo. The crude product was dissolved in a small amount of CHCl_3 and precipitated with diethyl ether. Flash chromatography on silica gel-*H* ($d = 3$ cm, $l = 25$ cm) with a $\text{CHCl}_3/\text{MeOH}$ gradient from 7.5:1 to 5:1 afforded **4a** as an orange-colored powder (53 mg, 16%). R_f ($\text{CHCl}_3/\text{MeOH}/\text{HOAc}$, 5:1:1): 0.44. Mp: >250 °C. IR (KBr): 3414m, 3064w, 2951w, 2862w, 1700s, 1647s, 1605s, 1584m, 1538s, 1462m, 1410w, 1252m, 1228m, 1017w, 798w. ^1H NMR (500 MHz, $(\text{CD}_3)_2\text{SO}$): δ 0.84 (t, $J = 7.0$ Hz, 3 H), 0.86 (t, $J = 7.0$ Hz, 3 H), 1.28 (m, 8 H), 1.55 (m, 4 H), 2.37 (s, 3 H), 2.48 (s, 3 H), 3.45 (m, 4 H), 3.51 (d, $J = 16.7$ Hz, 1 H), 3.57 (d, $J = 16.7$ Hz, 1 H), 3.63 (m, 2 H), 3.85 (m, 4 H), 4.13 (d, $J = 16.5$ Hz, 1 H), 4.14 (m, 2 H), 4.19 (d, $J = 16.5$ Hz, 1 H), 4.58 (m, 2 H), 4.69 (m, 2 H), 5.44 (dd, $J = 12.2$ Hz, $J = 16.4$ Hz, 2 H), 7.21 (dd, $J = 2.0$ Hz, $J = 8.9$ Hz, 1 H), 7.37 (m, 1 H), 7.44 (m, 2 H), 7.54 (m, 2 H), 7.80 (s, 1 H), 7.89 (s, 1 H), 7.91 (s, 1 H), 8.11 (d, $J = 8.9$ Hz, 1 H), 8.34 (t, $J = 6.0$ Hz, 1 H), 8.59 (t, $J = 5.8$ Hz, 1 H), 8.91 (s, 1 H), 10.46 (s, 1 H), 10.48 (s, 1 H). ^{13}C NMR (125 MHz, $(\text{CD}_3)_2\text{SO}$) δ 13.72, 13.75, 18.62, 20.72, 21.76, 21.77, 26.89, 27.00, 28.51, 28.56, 35.38, 35.59, 38.80 (2C), 40.10, 40.78, 42.76, 42.77, 48.04, 48.19, 54.84, 55.06, 70.28, 99.56, 111.28, 115.12, 115.89, 115.99, 127.88 (2C), 128.15, 128.52 (2C), 130.79, 130.97, 133.58, 134.02, 135.79, 135.81, 136.10, 141.90, 142.39, 146.61, 148.88, 152.35, 152.42, 154.74, 155.67, 155.96, 159.20, 161.35, 164.40, 167.23, 167.25, 168.36, 168.79. HRMS (FAB) for $\text{C}_{56}\text{H}_{61}\text{N}_{13}\text{O}_{11}$: ($\text{M} + 1^+$) calcd 1092.4691, found 1092.4690.

General Method for the Debenzylation of the Model Compounds (Synthesis of 1b, 2b, 3b). The model compound (either **1a**, **2a**, or **3a**) was dissolved in acetic acid at room temperature (5 mL). A suspension of 10% Pd/BaSO₄ catalyst (5 mg) in acetic acid (0.5 mL) was added, and the reaction mixture was stirred for 30 h in an H_2 atmosphere (1 bar). The mixture was filtered through Celite, and the filtrate was evaporated in vacuo to dryness. The obtained material was investigated by fluorescence and UV-visible spectroscopy. The purity was determined by analytical reversed-phase HPLC (RP18-column with a H_2O (1% TFA)/ CH_3CN gradient, 100% water to 100% acetonitrile over 100 min).

For the synthesis of **4b**, compound **4a** (20 mg, 0.018 mmol) was debenzylated, and the model compound **4b** was isolated by preparative reversed-phase HPLC (RP18-column with a H_2O (1% TFA)/ CH_3CN gradient, 100% water to 100% acetonitrile over 100 min) as a green-colored powder (18 mg, 99%). Mp: 253–255 °C. IR (KBr): 3436s, 2952w, 2922w, 2856w, 1700m, 1628m, 1600m, 1578m, 1546s, 1467m, 1267m, 1222w, 1201w, 1182w, 1156w, 1028w. ^1H NMR (500 MHz, $(\text{CD}_3)_2\text{SO}$): δ 0.85 (t, $J = 7.0$ Hz, 3 H), 0.86 (t, $J = 7.0$ Hz, 3 H), 1.30 (m, 8 H), 1.55 (m, 4 H), 2.39 (s, 3 H), 2.49 (s, 3 H), 3.42 (d, $J = 16.8$ Hz, 1 H), 3.45 (m, 4 H), 3.49 (d, $J = 16.8$ Hz, 1 H), 3.63 (m, 2 H), 3.85 (m, 4 H), 4.09 (m, 2 H), 4.13 (d, $J = 16.6$ Hz, 1 H), 4.15 (d, $J = 16.6$ Hz, 1 H), 4.60 (m, 4 H), 6.83 (m, 1 H), 7.03 (m, 1 H), 7.88 (m, 1 H), 7.92 (s, 1 H), 7.93 (s, 1 H), 8.40 (t, $J = 5.8$ Hz, 1 H), 8.44 (t, $J = 5.6$ Hz, 1 H), 8.69 (s, 1 H), 10.44 (s, 1 H), 10.45 (s, 1 H). ^{13}C

NMR (125 MHz, $(\text{CD}_3)_2\text{SO}$): δ 13.74, 13.76, 18.64, 20.76, 21.78 (2C), 26.91, 27.08, 28.51, 28.59, 35.54, 35.55, 38.53, 39.00, 40.15, 40.77, 42.82, 42.83, 47.98, 47.99, 54.69, 55.04, 100.75, 108.20, 114.70, 115.91, 130.86, 130.96, 133.84, 134.04, 135.79, 135.80, 136.16, 140.90, 143.80, 146.60, 148.91, 152.32, 152.39, 154.77, 155.87, 155.88, 159.26, 161.73, 163.90, 167.17, 167.32, 168.05, 168.34. HRMS (FAB) for $\text{C}_{49}\text{H}_{55}\text{N}_{13}\text{O}_{11}$: ($\text{M} + 1^+$) calcd 1002.4222, found 1002.07.

Model Compound 3a. BOP (210 mg, 0.452 mmol) was added to a solution of the *cis-syn*-biscarboxymethyluracil dimer **6** (70 mg, 0.21 mmol) in DMF (8 mL). This solution was stirred for 10 min at room temperature. A solution of the deazaflavin peptide **13** (130 mg, 0.21 mmol) dissolved in DMF (7 mL) was then added together with ca. 15 drops of NEt_3 . The solution was stirred for 90 min at room temperature. An excess of the aminoethyl-flavin **8** (100 mg, 0.29 mmol) dissolved in DMF (5 mL) was added, and the solution was stirred for another 90 min at room temperature. The reaction mixture was concentrated to ca. 15 mL. This solution was subjected to reversed-phase HPLC (RP18-column with a H_2O (1% TFA)/ CH_3CN gradient from 100% water to 100% acetonitrile over 100 min). The model compound **3a** was obtained as an orange-colored powder (60 mg, 32%). Mp: 232–234 °C. IR (KBr): 3423s, 3067w, 2967w, 2878w, 1700s, 1646s, 1606s, 1585m, 1537s, 1459m, 1417w, 1372w, 1333w, 1254m, 1228m, 1189w, 1017w. NMR gave broad, unresolved signals. HRMS (FAB) for $\text{C}_{60}\text{H}_{62}\text{N}_{16}\text{O}_{14}$: ($\text{M} + 1^+$) calcd 1231.4709, found 1231.4707.

Model Compound 2a. BOP (270 mg, 0.581 mmol) was added to a solution of the *cis-syn*-biscarboxymethyluracil dimer **6** (90 mg, 0.27 mmol) in DMF (8 mL). This solution was stirred for 10 min at room temperature. Then a solution of the deazaflavin peptide **14** (220 mg, 0.27 mmol) dissolved in DMF (7 mL) was added together with ca. 20 drops of NEt_3 . The solution was stirred for 90 min at room temperature. An excess of the aminoethyl-flavin **8** (130 mg, 0.37 mmol) dissolved in DMF (5 mL) was added, and the solution was stirred for another 3 h at room temperature. The reaction mixture was concentrated to ca. 10 mL. This solution was subjected to reversed-phase HPLC (RP18-column with a H_2O (1% TFA)/ CH_3CN gradient from 100% water to 100% acetonitrile over 100 min). The model compound **2a** was obtained as an orange-colored powder (5 mg, 1%). Mp: 266–268 °C. IR (KBr): 3450s, 2967w, 2878w, 1700s, 1629s, 1583s, 1546s, 1455m, 1428w, 1367w, 1336m, 1261w, 1229s, 1056w, 1017w, 922w. NMR gave broad, unresolved signals. HRMS (FAB) for $\text{C}_{70}\text{H}_{76}\text{N}_{18}\text{O}_{16}$: ($\text{M} + 1^+$) calcd 1425.5765, found 1425.5790.

Model Compound 1a. A solution of the flavin–deazaflavin peptide **27** (120 mg, 0.122 mmol) in DMF (6 mL) was stirred after the addition of a solution of 40% dimethylamine in H_2O (2 mL) for 20 min at room temperature. This solution was evaporated to dryness in vacuo, and the remaining amine **12** (93 mg, quantitative) was dried under high vacuum. A solution of the *cis-syn*-biscarboxymethyluracil dimer **6** (50 mg, 0.15 mmol) and BOP (150 mg, 0.323 mmol) in DMF (6 mL) was prepared and stirred for 10 min at room temperature. This solution was added to the solution of the amine **12** (93 mg, 0.122 mmol) in DMF (5 mL). Ten drops of NEt_3 were added, and the reaction mixture was stirred for 30 min at room temperature. An excess of 1-pentylamine was added, and the reaction mixture was stirred for another 2 h. The solution was diluted with CHCl_3 (100 mL) and washed three times with H_2O (3×100 mL). The organic phase was dried over MgSO_4 , filtered, and concentrated in vacuo to dryness. The obtained material was dissolved in a small amount of CHCl_3 and precipitated with Et_2O . The solid material was filtered off and obtained after column chromatography on silica gel-*H* ($d = 3$ cm, $l = 20$ cm, with a $\text{CHCl}_3/\text{MeOH}$ gradient from 10:1 to 7:1) as an orange powder (28 mg, 20%). R_f ($\text{CHCl}_3/\text{MeOH}$, 10:1): 0.19. Mp: 227–229 °C. IR (KBr): 3436s, 3078w, 2950w, 2933w, 2856w, 1689s, 1644s, 1604s, 1578m, 1538s, 1463m, 1406w, 1372w, 1247m, 1228m, 1211w, 1183w, 1156w, 1017w. ^1H NMR (500 MHz, $(\text{CD}_3)_2\text{SO}$): δ 0.84 (t, $J = 7.1$ Hz, 3 H), 0.86 (t, $J = 7.1$ Hz, 3 H), 1.25 (m, 8 H), 1.36 (m, 2 H), 1.54 (m, 2 H), 2.44 (s, 3 H), 2.55 (s, 3 H), 3.00 (q, $J = 6.9$ Hz, 2 H), 3.38 (d, $J = 16.5$ Hz, 1 H), 3.46 (m, 2 H), 3.47 (d, $J = 16.5$ Hz, 1 H), 3.50 (m, 2 H), 3.65 (m, 2 H), 3.84 (t, $J = 7.3$ Hz, 2 H), 4.05 (m, 1 H), 4.11 (m, 1 H), 4.13 (d, $J = 16.4$ Hz, 1 H), 4.15 (d, $J = 16.4$ Hz, 1 H), 4.52 (s, 2 H), 4.63 (m, 1 H), 4.64 (m, 2 H), 4.74 (m, 1 H), 5.40 (s, 2 H), 7.23 (dd, $J = 2.0$ Hz, $J = 8.9$ Hz, 1 H), 7.31 (m, 3 H), 7.48 (d, $J = 6.9$ Hz, 2 H), 7.77

(s, 1 H), 7.92 (t, $J = 5.6$ Hz, 1 H), 7.97 (s, 1 H), 8.00 (s, 1 H), 8.14 (d, $J = 8.9$ Hz, 1 H), 8.34 (t, $J = 5.8$ Hz, 1 H), 8.61 (t, $J = 5.8$ Hz, 1 H), 8.93 (s, 1 H), 10.39 (s, 1 H), 10.43 (s, 1 H). ^{13}C NMR (125 MHz, $(\text{CD}_3)_2\text{SO}$): δ 13.76, 13.78, 18.70, 20.82, 21.70, 21.77, 26.99, 28.43, 28.55, 28.66, 35.30, 35.69, 38.27, 38.40, 38.93, 40.08, 42.92, 43.04, 43.78, 48.04, 48.16, 54.55, 55.17, 70.29, 99.49, 111.23, 115.20, 115.98, 116.06, 128.12 (2C), 128.25, 128.37 (2C), 130.74, 131.09, 133.55, 134.06, 135.76, 136.13, 136.24, 141.95, 142.56, 147.11, 149.09, 152.31, 152.34, 154.53, 155.63, 155.90, 159.36, 161.40, 164.49, 166.87, 167.13, 167.44, 168.31, 168.38. HRMS (FAB) for $\text{C}_{58}\text{H}_{64}\text{N}_{14}\text{O}_{12}$: ($\text{M} + 1^+$) calcd 1149.4906, found 1149.4899.

Splitting Assay. For the repair assay, all model compounds were dissolved in ethylene glycol at 10^{-6} M concentration, and the solution was vigorously degassed. Addition of a sodium dithionite solution (0.05 M in water) and 10 μL of NEt_3 converted the flavin moiety in all model compounds into the reduced and deprotonated form. The cuvettes were placed in a fluorescence spectrometer and irradiated with a monochro-

matic light beam at the specified wavelengths. During an experiment, $6 \times 50\text{-}\mu\text{L}$ aliquots of the assay solution were removed, immediately reoxidized by the addition of oxygen, and analyzed by reversed-phase HPLC (Nucleogel C18-column, water/methanol gradient). Integration of the product and the starting material peaks yielded the reaction rate per minute. The number of absorbed light quanta per minute was determined by ferrioxalate actinometry. Both values were used to calculate the quantum yield Φ (= number of reacted molecules/number of absorbed photons). Φ is a measure of the efficiency of the overall light energy conversion.

Acknowledgment. This work was supported by the Swiss National Science Foundation. We thank Prof. F. Diederich for his very generous support.

JA990466L